DOE/NV/03624--1220

Data Release Report for the Source Physics Experiment Phase II: Dry Alluvium Geology Experiments (DAG-1 through DAG-4) Nevada National Security Site

October 2021

Compiled by:
Jennifer Larotonda and Margaret Townsend
Mission Support and Test Services, LLC

With contributions from:

Lawrence Livermore National Laboratory
Gene Ichinose, Robert Mellors, and William R. Walter

Los Alamos National Laboratory
Ting Chen, Michael Malone, Steven Pemberton, Emily Schultz-Fellenz, and Juan-Antonio Vigil

Sandia National Laboratories
Robert Abbott, Daniel Bowman, Avery "Zack" Cashion, and David Yocky

Nevada Seismology Laboratory, University of Nevada, Reno
Gabriel Plank and Kenneth Smith

Mission Support and Test Services, LLC
Rand Kelly, Kale McLin, and Cleat Zeiler

NNSS Weather Operations, Air Resources Laboratory/Special Operations & Research Division
Walter Schalk

This work was done by Mission Support and Test Services, LLC under Contract No. DE-NA0003624 with the U.S. Department of Energy, and the Office of Defense Nuclear Nonproliferation Research and Development.
DOE/NV/03624--1220

DISCLAIMER STATEMENT

AVAILABILITY STATEMENT

Available for sale to the public, in paper, from–

U.S. Department of Commerce
National Technical Information Service
5301 Shawnee Road
Alexandria, VA 22312
Telephone: 800.553.6847
Fax: 703.605.6900
E-mail: orders@ntis.gov
Online ordering: http://www.ntis.gov/help/ordermethods.aspx

Available electronically at http://www.osti.gov/bridge

Available for a processing fee to U.S. Department of Energy and its contractors, in paper, from–

U.S. Department of Energy
Office of Scientific and Technical Information
P.O. Box 62
Oak Ridge, TN 37831-0062
Telephone: 865.576.8401
Fax: 865.576.5728
E-mail: reports@adonis.osti.gov

DOE/NV/03624--1220

Data Release Report for the Source Physics Experiment Phase II: Dry Alluvium Geology Experiments (DAG-1 through DAG-4) Nevada National Security Site

Compiled by:

Jennifer Larotonda and Margaret Townsend
Mission Support and Test Services, LLC

With contributions from:

Lawrence Livermore National Laboratory
Gene Ichinose Robert Mellors William R. Walter

Los Alamos National Laboratory
Ting Chen Michael Malone Steven Pemberton Emily Schultz-Fellenz Juan-Antonio Vigil

Sandia National Laboratories
Robert Abbott Daniel Bowman Avery "Zack" Cashion David Yocky

N**evada Seismology Laboratory, University of Nevada, Reno**
Gabriel Plank Kenneth Smith

Mission Support and Test Services, LLC
Rand Kelly Kale McLin Cleat Zeiler

NNSS Weather Operations, Air Resources Laboratory/Special Operations and Research Division
Walter Schalk

October 2021

Assembled data sets are accessible through:
Incorporated Research Institutions for Seismology
Data Management Center
1408 NE 45th Street, Suite 201
Seattle, Washington 98105 USA
www.iris.washington.edu

Report Citation Reference: Mission Support and Test Services, LLC, 2021. *Data Release Report for Source Physics Experiment Phase II: Dry Alluvium Geology Experiments (DAG-1 through DAG-4), Nevada National Security Site.* Technical Report DOE/NV/03624--1220, 85 pages. Las Vegas, NV

Source Physics Experiment Phase II – Dry Alluvium Geology

Principal Investigators:

Lawrence Livermore National Laboratory

Souheil Ezzedine, Sean Ford, Gene Ichinose, Robert Mellors, William R. Walter

Los Alamos National Laboratory

Ray Guffee, Carene Larmat, Gordon MacLeod, Catherine M. Snelson, David Steedman

Sandia National Laboratories

Robert Abbott, Daniel Bowman, Scott Broome, Avery "Zack" Cashion, David Yocky

Air Force Technical Applications Center

Chandan Saikia

Nevada Seismological Laboratory, University of Nevada, Reno

Gabriel Plank, Kenneth Smith

Mission Support and Test Services, LLC

Jesse Bonner, Cleat Zeiler

Other Major Contributors:

Lawrence Livermore National Laboratory

Tarabay Antoun, Justin Barno, Andrea Chiang, Doug Dodge, Beth Dzenitis
Terri Hauk, Keehoon Kim, Doug Knapp, Kayla Kroll, J. P. Lewis
Steven Magana-Zook, Eric Matzel, Steve Myers, Michael Pasyanos, Arben Pitarka
Moira Pyle, Rebecca Rodd, Artie Rodgers, Rich Rose, Oleg Vorobiev
Jeff Wagoner

Los Alamos National Laboratory

Lewis Allen, Philip Blom, Michelle Bourret, Christopher Bradley, Ting Chen
K. Michael Cleveland, David Coblentz, Adam Collins, Brandon Crawford, Julian Dann
Fransiska Dannemann, Andrew Delorey, Peter Dickson, Garrett Euler, Robert Gentzlinger
Joel Heidemann, Alexandra Iezzi, Earl Knight, Ken Laintz, Emma Lathrop
Anita Lavadie-Bulnes, Pierre-Yves Le Bas, Zhou Lei, Daniel Livingston, Michael Malone
Damien Milazzo, Elizabeth Miller, Terry Miller, Dea Musa, Howard Patton
Steven Pemberton, W. Scott Phillips, Esteban Rougier, Charlotte Rowe, Thomas Sandoval
Emily Schultz-Fellenz, Gerald Seitz, Kurt Solander, Richard Stead, Erika Swanson
Ellen Syracuse, Scott Traeger, Juan-Antonio Vigil, Jeremy Webster, Rodney Whitaker
Xiaoning Yang

Sandia National Laboratories

Sarah Albert, Jonah Bartrand, Andrea Darrh, Jason P.Garland, Austin Holland
Charles Hoots, Richard Jensen, Emily Morton, Christian Poppeliers, Leiph Preston
Rosamiel Ries, Jiann Su, Liam Toney, Derek West, Lauren Wheeler
Brian Young

Mission Support and Test Services, LLC

Sigmund Drellack, Veraun Chipman, Bryan Eleogram, Michael Hanache, Kaleb Howard
Heather Huckins-Gang, Rand Kelly, Jennifer Larotonda, Kale McLin, Curtis Obi
Lance Prothro, Margaret Townsend, Karl Wagner, James Wilson, Robert White

NNSS Weather Operations, Air Resources Laboratory/Special Operations and Research Division

Walter Schalk

Silixa, LLC

Thomas Coleman, Taylor Martin

Executive Summary

The Dry Alluvium Geology (DAG) project was Phase II of the Source Physics Experiment and consisted of a series of four chemical explosive tests conducted in the same source hole on the Nevada National Security Site. This hole is located at 37.1146°N and -116.0693°W, with a surface elevation of 1,285.2 meters (m) (4,216.5 feet [ft]) above sea level.

The first test (DAG-1) was conducted on July 20, 2018, at 16:51:52.67838 Coordinated Universal Time (UTC). The explosive source for DAG-1 was nitromethane initiated by a small plastic-bonded explosive (PBX) charge, detonated at the depth of 385.0 m (1,263.2 ft) below ground surface. DAG-1 had a trinitrotoluene (TNT) equivalent yield of 0.908 metric tons (2,002 pounds [lbs]).

DAG-2 was conducted on December 19, 2018, at 18:45:56.92115 UTC. This test was the largest in the series, with a TNT equivalent yield of 50.997 metric tons (112,429 lbs). The explosive source for DAG-2 was nitromethane initiated by a small PBX charge, detonated at the depth of 299.8 m (983.6 ft) below ground surface.

DAG-3 was conducted on April 27, 2019, at 15:49:01.84183 UTC. The explosive source for this test was nitromethane initiated by a small PBX charge, detonated at the depth of 149.9 m (492.0 ft) below ground surface. DAG-3 had a TNT equivalent yield of 0.908 metric tons (2,002 lbs).

The final DAG test (DAG-4) was conducted on June 22, 2019, at 21:06:19.87632 UTC. The explosive source for DAG-4 was nitromethane initiated by a small PBX charge, detonated at the depth of 51.6 m (169.3 ft) below ground surface. DAG-4 had a TNT equivalent yield of 10.357 metric tons (22,833 lbs).

The four tests were recorded by an extensive set of instrumentation that included sensors both at near-field (less than 200 m) and far-field (200 m or greater) distances. The near-field instruments consisted of three-component (3C) accelerometers installed at various depths ranging from 51.6 to 385 m (169.3 to 1,263.1 ft) below ground surface in boreholes positioned around the source hole, and arrays of single-component and 3C accelerometers on the surface. The far-field network comprised a variety of seismic and acoustic sensors, including short-period geophones, broadband seismometers, and 3C accelerometers at distances of 200 m to 400 kilometers. In addition, the DAG-2, DAG-3, and DAG-4 explosions were recorded by a temporary array of 496 geophones arranged in a densely spaced grid pattern known as “Large N.”

This report coincides with the release of these data for analysts and organizations that are not participants in this program. This report describes the four DAG tests and the various types of near-field, far-field, and other data that are available. Assembled data sets are accessible through:

Incorporated Research Institutions for Seismology, Data Management Center
1408 NE 45th Street, Suite 201, Seattle, Washington 98105 USA.
www.iris.washington.edu

Description: Dry Alluvium Geology experiments 1 through 4 to study the generation and propagation of seismic waves from underground explosions.

Full Name	Nickname	ID
Dry Alluvium Geology 1	DAG-1	21-020
Dry Alluvium Geology 2	DAG-2	21-021

Full Name	Nickname	ID
Dry Alluvium Geology 3	DAG-3	21-022
Dry Alluvium Geology 4	DAG-4	21-023

This page intentionally left blank.

Table of Contents

Table of Contents (cont.)

List of Appendices

List of Attachments

List of Figures

List of Tables

List of Acronyms and Abbreviations

3C	three-component
AFTAC	Air Force Technical Applications Center
Corrtex	COntinuous Reflectometry for Radius vs. Time Experiment
DAG	Dry Alluvium Geology
EM	electromagnetic
FDSN	Federation of Digital Seismic Networks
ft	foot (feet)
GPS	global positioning system
HWC	helically wound cable
Hz	hertz
in.	inch(es)
IRIS	Incorporated Research Institutions for Seismology
kHz	kilohertz
km	kilometer(s)
LANL	Los Alamos National Laboratory
lbs	pounds
LLNL	Lawrence Livermore National Laboratory
m	meter(s)
MSTS	Mission Support and Test Services, LLC
NNSS	Nevada National Security Site
NSL	Nevada Seismological Laboratory
NSTec	National Security Technologies, LLC
PBX	plastic-bonded explosive
PolSAR	Fully Polarimetric Synthetic Aperture Radar Imagery
SEED	Standard for the Exchange of Earthquake Data
SGZ	surface ground zero
SNL	Sandia National Laboratories
SORD	NNSS Weather Operations, Air Resources Laboratory/Special Operations and Research Division
SPE	Source Physics Experiment
sps	samples per second
TD	total depth
TNT	trinitrotoluene
UNR	University of Nevada, Reno
UTC	Coordinated Universal Time

This page intentionally left blank.

1 Introduction

The Dry Alluvium Geology (DAG) project was Phase II of the Source Physics Experiment (SPE) and consisted of a series of four chemical explosive tests (Snelson et al. 2019). The test bed was constructed in alluvium in northern Yucca Flat at the Nevada National Security Site (NNSS; formerly known as the Nevada Test Site) starting in 2016 (Figure 1). These tests were sponsored by the U.S. Department of Energy, National Nuclear Security Administration's Office of Defense Nonproliferation Research and Development. The DAG test series was primarily designed to study the generation and propagation of seismic waves, and provided data that will improve the predictive capability of numerical models for detecting and characterizing underground explosions (e.g., Ford and Walter 2013; Snelson et al. 2012; 2013; 2019). These validated, improved seismic-acoustic models and simulations will enhance the U.S. ability to detect and discriminate low-yield nuclear explosions.

The DAG tests were designed and conducted by a consortium of organizations, including Lawrence Livermore National Laboratory (LLNL), Los Alamos National Laboratory (LANL), and Sandia National Laboratories (SNL), in conjunction with Mission Support and Test Services, LLC (MSTS). The University of Nevada, Reno (UNR) assisted in data acquisition and compilation. Other organizations, including the Air Force Technical Applications Center (AFTAC) and Silixa, LLC, also participated in data acquisition efforts.

The execution dates for the DAG tests are listed below.

- DAG-1: July 20, 2018
- DAG-2: December 19, 2018
- DAG-3: April 27, 2019
- DAG-4: June 22, 2019

The vast majority of data acquired under the DAG program are unclassified/unlimited but subject to a 2-year hold, similar to the policy of the U.S. National Science Foundation. This report presents information that will aid in the understanding and proper use of the DAG data sets.

Cleat Zeiler, MSTS point of contact (zeilercp@nv.doe.gov), can be contacted for further information, including information about other data collected at the DAG site.

2 Test Objectives

The objectives for the three phases of the SPE Source Physics series are described in the overall Science Plan (Snelson et al. 2019). Similar to the SPE Phase 1 experiments, the DAG experiments consisted of a series of chemical explosions conducted at different depths, in the same geologic medium (alluvium, considered a "weak rock"), all at the same geographic location. Each of the four DAG explosive tests was recorded on the same sensor layout, although as the test sequence progressed, additional sensors were added.

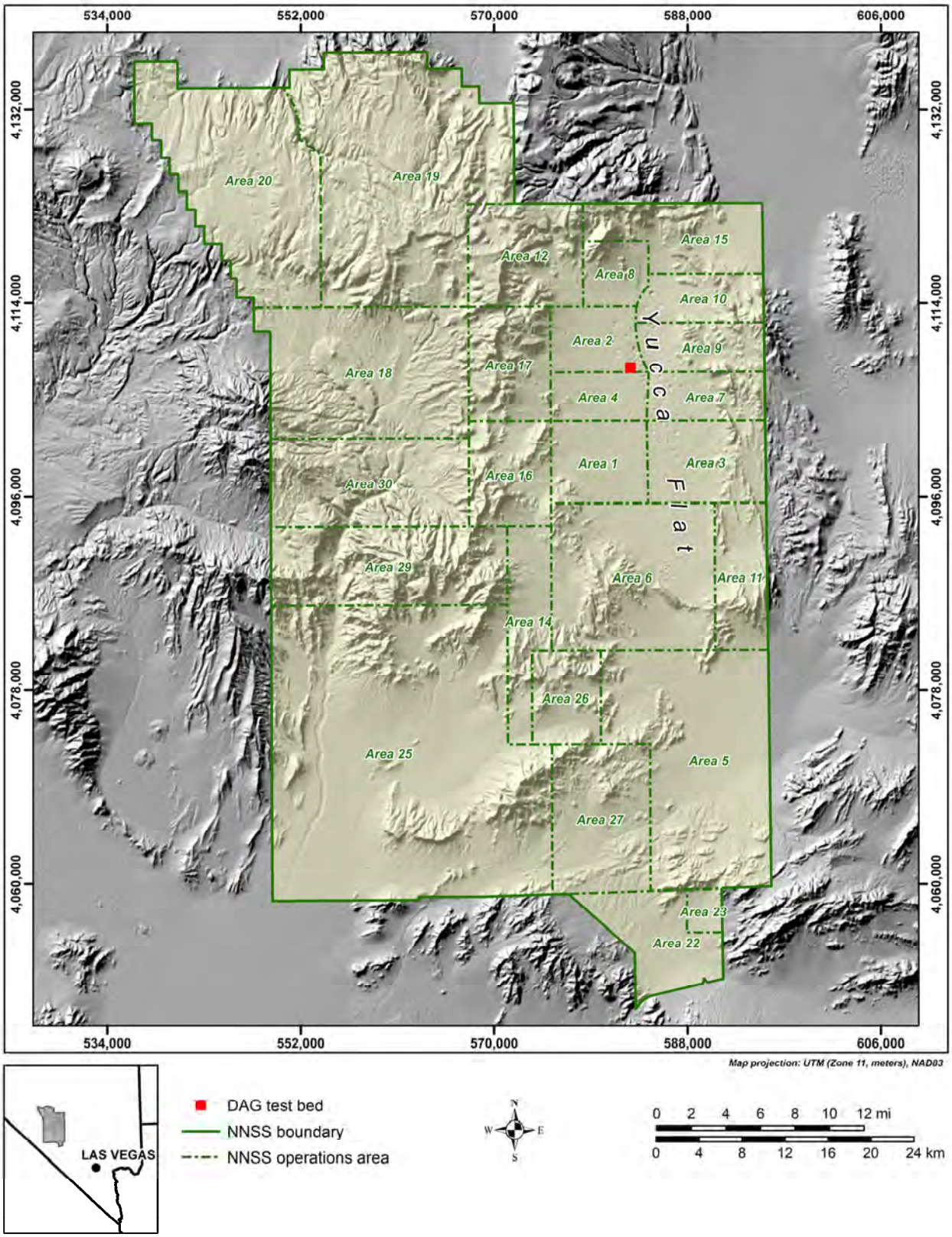

Figure 1
Reference Map Showing the Location of the DAG Test Bed at the Nevada National Security Site

The DAG series provided new explosion signature data from a wide range of diagnostic equipment (e.g. seismic, acoustic, electromagnetic surface photogrammetry, etc.). These data will be compared with data from the SPE Phase I, conducted in a granite test bed, as well as with nearby historic nuclear test data for explosions in alluvium and other materials, and will allow the development, testing, and validation of new empirical and physics-based modeling computational codes. Analysis of the Phase II DAG data is underway as noted in several recent studies (e.g., Blom et al. 2020; Ichinose et al. 2021).

Several analyses of SPE Phase I data have been published (e.g., Bowman 2019; Chen et al. 2020; Ford and Vorobiev 2020; Ford and Walter 2021; Pasyanos and Kim 2019; Pitarka and Mellors 2021; Poppeliers et al. 2020; Preston et al. 2020; Pyle and Walter 2019; Scalise et al. 2021; Schultz-Fellenz et al. 2020; Swanson et al. 2020; Vorobiev and Rubin 2021a; 2021b; Yocky et al. 2021).

2.1 Summary of DAG Test Design Information

Information about the DAG tests is summarized in Table 1, and described in the following paragraphs.

2.2 DAG-1

The DAG-1 test was conducted in the U-2ez source hole, with a trinitrotoluene (TNT) equivalent yield of 0.908 metric tons (2,002 pounds [lbs]) set at the depth of 385.0 meters (m) (1,263.2 feet [ft]). DAG-1 was an initial Green's Function test designed to establish direct measurement of the explosive source in weak rock geology and emplaced as deep as reasonable to minimize spall. It was analogous to SPE-4Prime (National Security Technologies, LLC [NSTec] 2017). See a detailed description of the source in Section 4.1.

2.3 DAG-2

The DAG-2 test was the largest in the series of tests at the U-2ez location, with a TNT equivalent yield of 50.997 metric tons (112,429 lbs) set at the depth of 299.8 m (983.6 ft) in the source hole. The objective of the DAG-2 test was to generate regional signals to 300 kilometers (km), analogous to those of SPE-5 (MSTS 2019), for comparison with monitoring stations that recorded historical nuclear tests. See a detailed description of the source in Section 4.2.

Table 1
Information for the Dry Alluvium Geology Experiments 1 through 4 (DAG-1 through DAG-4)

Surface Location: 37.114644234, -116.06926431		**Surface Elevation:** 1,285.2 m (4,216.5 ft)	
	DAG-1	**DAG-2**	**DAG-3**	**DAG-4**
Date	07/20/2018 (Day 201)	12/19/2018 (Day 353)	04/27/2019 (Day 117)	06/22/2019 (Day 173)
Time (Coordinated Universal Time)	16:51:52.67838	18:45:56.92115	15:49:01.84183	21:06:19.87632
TNT Equivalent Yield (metric tons)	0.908	50.997	0.908	10.357
TNT Equivalent Yield (lbs)	2,002	112,429	2,002	22,833
Depth	385.0 m (1,263.2 ft)	299.8 m (983.6 ft)	149.9 m (492.0 ft)	51.6 m (169.3 ft)

2.4 DAG-3

The DAG-3 test was conducted in the U-2ez source hole, with a TNT equivalent yield of 0.908 metric tons (2,002 lbs) set at the depth of 149.9 m (492.0 ft). DAG-3 was a middle depth test conducted to compare to DAG-1, and serve as a Green's Function test for Large-N (a dense geophone network). It was analogous to SPE-1 (NSTec 2014). See a detailed description of the source in Section 4.3.

2.5 DAG-4

The DAG-4 test was conducted in the U-2ez source hole, with a TNT equivalent yield of 10.357 metric tons (22,833 lbs) set at the depth of 51.6 m (169.3 ft). The objective of the DAG-4 test was to provide data for comparison of a "normal-depth" explosion (i.e., similar in scaled depth of burial to historic underground nuclear explosive test) to the "over-buried" DAG explosions (DAG-1 through DAG-3) and was analogous to SPE-6 (MSTS 2019). See a detailed description of the source in Section 4.4.

2.6 Data Sets

A comprehensive set of strong-motion and seismo-acoustic instrumentation was deployed for the four tests. The near-field (<200 m from the shot point) instrumentation included high-sample-rate, three-component (3C) accelerometers deployed in boreholes. Single-component and 3C accelerometers were also installed at the surface for each test. At distances at and beyond 200 m (far-field), a large number of seismic and acoustic sensors were deployed at distances up to 400 km, including some of the exact locations at which the seismic signals from historic nuclear tests had been recorded. In addition to seismic data, the DAG team collected data from acoustic and infrasound sensors, high-speed video, and other instrumentation. A temporary deployment of 496 3C geophones (known as Large N), was installed in a grid sited 200 to 2,500 m from the test location, as were two dense lines with a spacing of 50 m along the southwest and southeast directions.

The following sections of this report provide more detailed information for these data sets. The data and metadata were compiled, archived, and distributed by the technical members of the Nevada Seismological Laboratory (NSL) at UNR. Records for stations at greater distances are available from the permanent UNR seismic network.

The full data sets for all four DAG tests, along with associated metadata, are available from the Incorporated Research Institutions for Seismology (IRIS) Data Management Center. This report is intended to complement the data sets and provide ancillary information.

Assembled data sets are accessible through:

> Incorporated Research Institutions for Seismology, Data Management Center
> 1408 NE 45th Street, Suite 201, Seattle, Washington 98105 USA.
> *www.iris.washington.edu*

Full Name	Nickname	ID
Dry Alluvium Geology 1	DAG-1	21-020
Dry Alluvium Geology 2	DAG-2	21-021

Full Name	Nickname	ID
Dry Alluvium Geology 3	DAG-3	21-022
Dry Alluvium Geology 4	DAG-4	21-023

3 Site Description

The DAG test bed consists of a cleared pad in an open and flat area in northern Yucca Flat. There is minimal fill across the pad surface and the substrate is alluvium (Figure 2). Twelve instrumentation holes were drilled in an array surrounding preexisting Inventory Emplacement Hole U-2ez (simply U-2ez in this report), which was selected to be the source hole for the DAG test series. See sections 3.1.2 and 5.1 for additional information about the instrument holes and sensors installed in them.

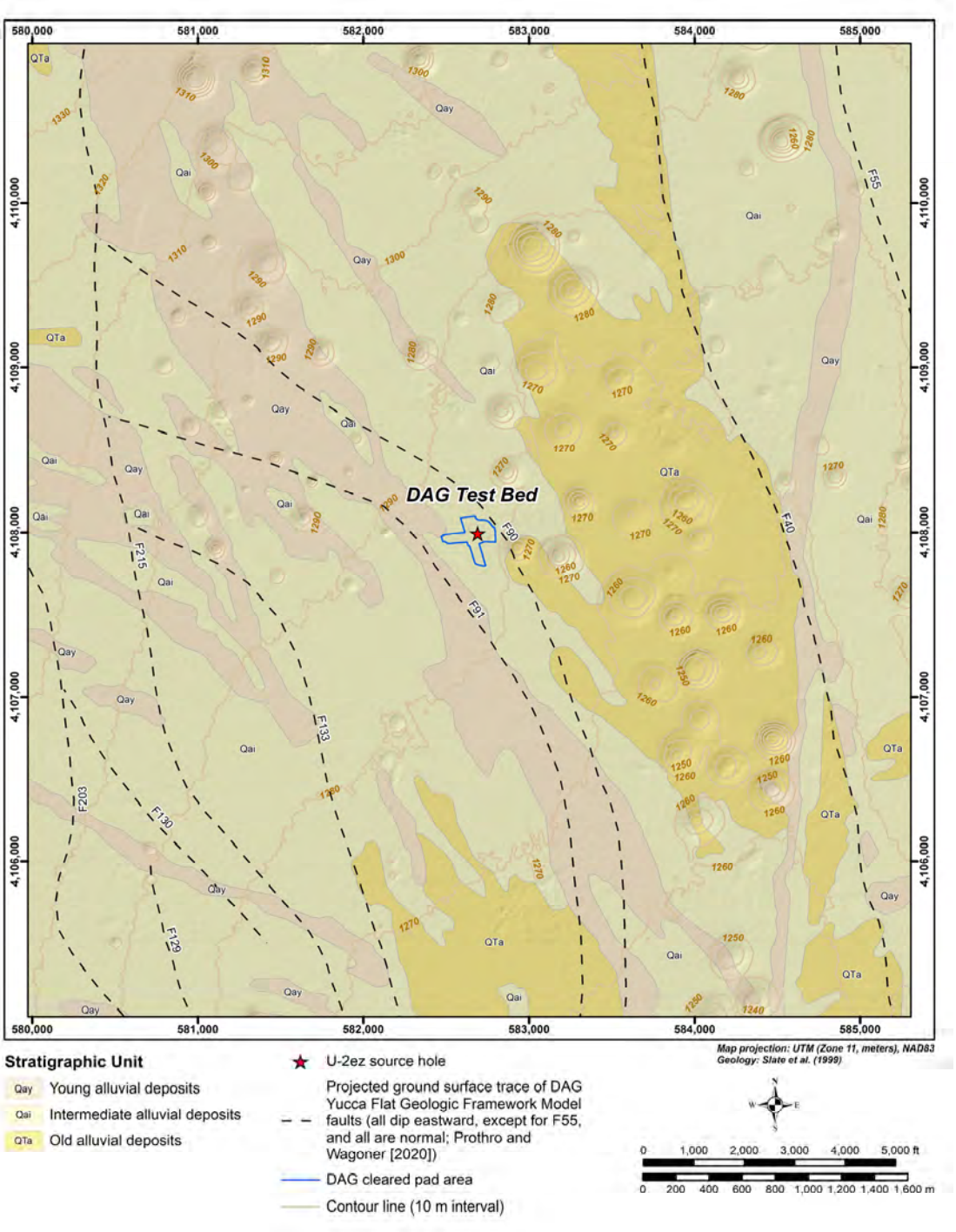

Figure 2
Map Showing the Surface Geology and Terrain of the DAG Test Bed

3.1 Test Bed Construction

3.1.1 Source Hole

Inventory Emplacement Hole U-2ez was drilled with a 2.44-m (8-ft) diameter bit to a total depth (TD) of 396.2 m (1,300 ft), in 1983. The borehole remained unused until it was selected for the DAG experiments. It was chosen based on its desirable alluvium characteristics, total depth, stability, and location. The four DAG tests were conducted in U-2ez at increasingly shallow depths by successively emplacing stemming following each test. No additional deepening of the source hole was needed.

3.1.2 Instrumentation Holes

To measure the response of the subsurface medium to the DAG explosions, a three-arm array of instrumentation holes was drilled in 2017 for later installation of diagnostic instruments. Each arm of the array has four holes spaced 10, 20, 40, and 80 meters from the source hole. Each hole was drilled to approximately 405 m (1,330 ft) into alluvium using a 10⅝-inch [in.] diameter tricone bit, except U-2ez-SW80, which was drilled to 518 m (1,700 ft) into the underlying volcanic tuff. Appendix 1 provides a summary of construction data for the U-2ez source hole and instrument holes. Figure 3 shows an aerial view of the DAG test bed with the locations of the source hole and instrument holes. See additional discussion of the near-field data in Section 5.1.

3.2 Geology

The location of the DAG test bed was selected based on the availability of an open, unused, large diameter borehole drilled in alluvium. The alluvium at the test bed is dry, soft, homogenous, and unfractured and is considered a weak rock. Because the existing borehole was originally constructed in preparation for an underground nuclear test in a commonly used testing area of the NNSS, abundant geologic, seismic, and ground shock data are available for comparison to DAG test data.

3.2.1 Geologic Setting

The following paragraphs are from the completion report for the DAG instrumentation holes (e.g., Wagner et al. 2017).

The DAG test bed lies in a north-trending graben that hosts Yucca Flat. Highlands around the valley are composed of Proterozoic and Paleozoic sedimentary rocks, Mesozoic intrusive rocks, and Cenozoic volcanic rocks that shed sediment into the alluvial basin. Proterozoic to Paleozoic marine carbonate and siliciclastic rocks experienced significant Mesozoic shortening, most widely expressed at the NNSS as older east- to southeast-vergent thrust faults (e.g., Belted Range fault system) and slightly younger west- to northwest-vergent folds and thrust faults (e.g., CP Hills thrust; Cole and Cashman 1999). Mesozoic granodiorite and quartz monzonite make up the Climax and Gold Meadows stocks north of Yucca Flat. Cenozoic-age variably welded rhyolite tuffs crop out along the margins of Yucca Flat, and form the upper sequence of rocks that predate basin development (e.g., Sawyer et al. 1994; Slate et al. 1999). Yucca Flat is one of many north-oriented alluvium-filled grabens formed by east-west Neogene Basin and Range extension (basin initiation dated as >8.1 and <11.45 Million years ago; Marvin et al. 1989; Bechtel Nevada 2006). Basin development pervasively overprinted the structures in the area. The dominant faults in the basin are the east-dipping Carpetbag-Topgallant and Yucca normal fault systems.

The uppermost sequence of rocks and sediment deposits at the DAG test bed are indurated Neogene to Quaternary alluvial sands and gravels, which increase in volcanic detritus with depth (Wagoner and McKague 1985; Bechtel Nevada 2006; Huckins-Gang and Drellack 2016). The grain size of the alluvium can vary horizontally at scales of tens of meters or less, which makes this widespread unit difficult to generalize (Sweetkind and Drake 2007; Phelps et al. 2011; Cronkite-Ratcliff et al. 2012).

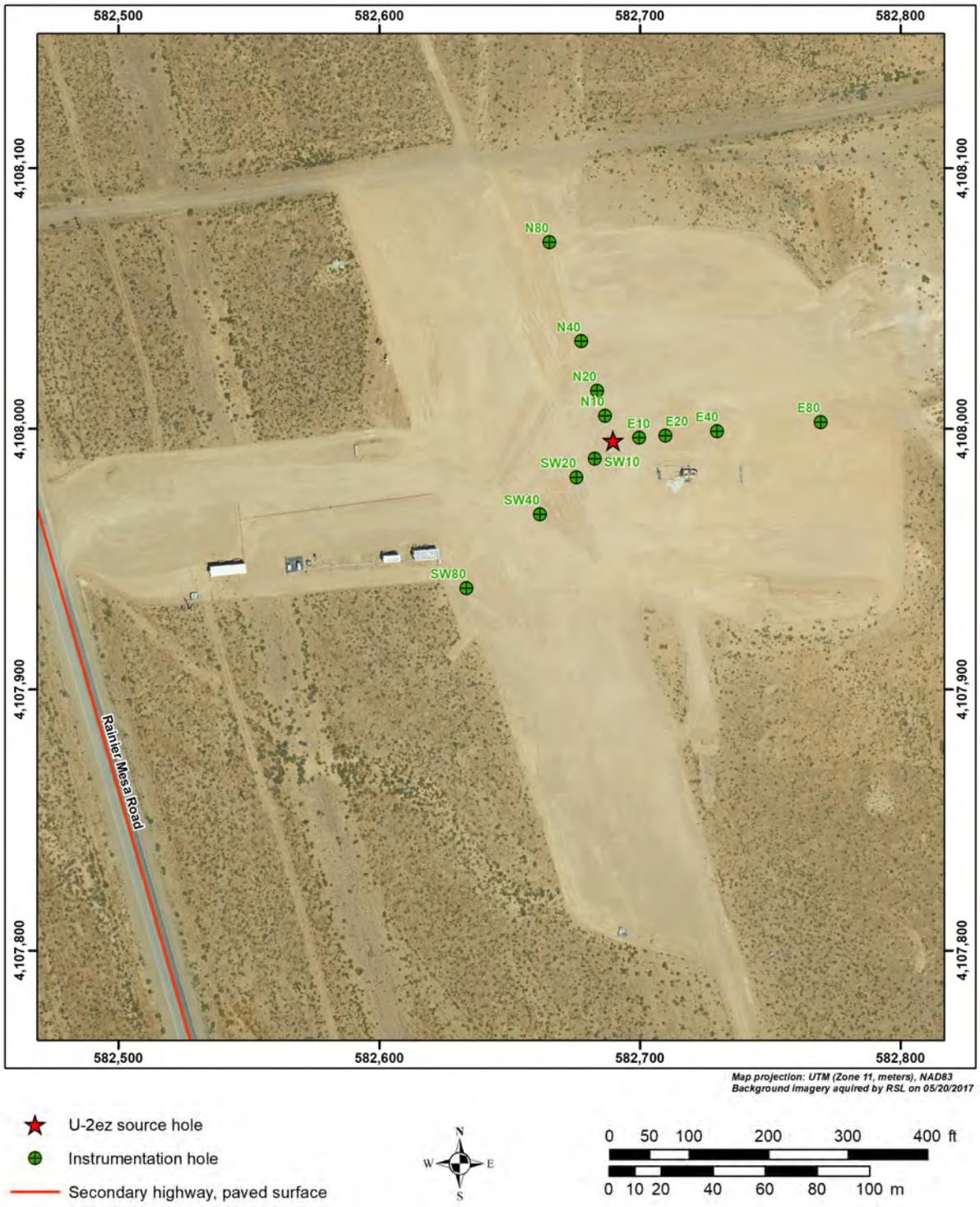

Figure 3
Aerial Photo of the DAG Test Bed Showing Locations of the Source Hole and Instrument Holes

In the U-2ez area, the alluvial deposits extend approximately 450 m (1,500 ft) below the surface, where they are in contact with variably welded volcanic tuffs of Neogene age. East-dipping normal faults buried just west of U-2ez, the emplacement hole for the experiments, suggest that the alluvial fill may be thinner near the west edge of the test bed (Howard 1980).

The static water level in Yucca Flat varies across the basin, but is deepest in the north; in the area around DAG, it is likely deeper than 500 m (1,750 ft). Depths to the underlying Proterozoic and Paleozoic basement rocks are poorly constrained in this part of the basin, but may lie as shallow as 900 m (3,000 ft) beneath the surface at U-2ez (Howard 1980).

Reconnaissance mapping of the near-surface geology at the DAG test bed indicates that there is minimal construction fill across the pad, and there are variable exposures of caliche on the pad surface (Huckins-Gang and Wagner 2017). Combined with ground disturbances from drilling and instrumentation (e.g., filled-in mud sumps and trenches, both historic and recent), this heterogeneity creates a complex surface that could complicate interpretation of surface effects and geophysical sensor responses to the experiments.

3.2.2 Geologic Characterization Data

The U-2ez source hole was drilled in 1983, prior to construction of the test bed. The twelve DAG instrumentation holes were drilled in 2017. During drilling, cuttings were collected from each borehole to characterize the geology. After drilling, a suite of geophysical logs and downhole camera runs were made in each borehole to characterize the geology, the borehole path, and borehole condition (e.g., areas with enlargement, ledges). Downhole camera runs and deviation surveys were also run in some of the instrumentation holes during drilling to assess hole conditions. The following sections describe the collected characterization data.

3.2.2.1 Source Hole

The drill crew collected cuttings at 3.0-m (10-ft) intervals from U-2ez during drilling. One-pint samples were collected from a bucket hanging from the drill-fluid exhaust pipe (“blooie line”) and are thus composites. No core samples were collected from the hole.

Geophysical logs collected from U-2ez after it was drilled in 1983 include caliper, density, resistivity, gamma, magnetic, neutron, and seismic. Two downhole videos were run to TD in 1988. Additional downhole videos collected by Colog, Inc. (February 12, 2014) and the U.S. Geological Survey (November 30, 2016), as well as a depth check by NSTec (August 22, 2017) show that the hole had eroded little since completion and had less than a few meters of fill.

3.2.2.2 Instrumentation Holes

The instrumentation holes were drilled in 2017. While augering the conductor holes from 0 to 26 m (0 to 85 ft) below ground surface, the drill crew collected samples of augered material at 3.1-m (10-ft) intervals for each hole except U-2ez-N10. These conductor hole samples are best considered spot samples. During drilling of each main hole, drill cuttings were collected by the drill crew at approximately 9.1-m (30-ft) intervals from the bottom of the conductor casing to TD. The drill crew collected a sample of cuttings at each kelly-down or shortly thereafter, during the connection of the

next joint of drill pipe. The samples from the main holes are best considered as representing a composite sample across the 9.1-m (30-ft) sample interval.

Downhole video camera runs were made with a GeoVision micro 500 camera before the casing was installed in the conductor holes at U-2ez-E80 and U-2ez-SW40 to document the shallow strata and borehole conditions. Additional video camera runs were done at U-2ez-SW40 to aid drillers in reconnecting to a dropped bottom-hole assembly, and at U-2ez-N40 to investigate borehole conditions that may have led to a drill bit getting stuck.

At U-2ez-N10, U-2ez-E10, and U-2ez-SW10 (the holes closest to the U-2ez emplacement hole), a REFLEX EZ-TRAC magnetic deviation tool was run downhole at every third connection (approximately 30-m [100-ft] intervals), without fully removing the drill pipe, to provide timely information on the borehole trajectory relative to emplacement hole U-2ez. This tool was operated by the drill crew and required adjustment of the bottom-hole assembly to accommodate non-magnetic, Monel alloy collars, which served as a target depth to record magnetic orientation measurements.

After drilling was completed, Colog, Inc. collected a suite of geophysical logs, which aided in assessing the condition of the boreholes and characterizing the geology. Geophysical logs run in each of the instrumentation holes include:

- Compensated formation density with one-armed caliper and gamma ray
- Optical televiewer with magnetic deviation
- Dual induction with natural gamma ray

NSTec recorded downhole video camera logs in U-2ez-SW20 and U-2ez-SW40 after drilling to assess borehole conditions. In addition, NSTec checked the total depths of all of the holes a few months after drilling with a weighted pipe attached to a wireline.

Inquiries about geologic characterization data should be directed to the MSTS point of contact, Cleat Zeiler (zeilercp@nv.doe.gov).

4 Test Descriptions

As described above, all four DAG tests were conducted in the same source hole, over a period of approximately eleven months. After each test, fill material was added to the hole to bury the underlying experiment debris, before the canister for the next test was inserted. Details for each test are provided in the following sections.

For all but DAG-4, the cable holding the previous test cannister were severed using small explosives prior to insertion of the next cannister. For the first three experiments of the series, acoustic sensors were in place for the experiment recorded these cable-cutter detonations.

Section 4.5 discusses detonation diagnostics for all four DAG tests.

4.1 Explosive Source and Detonation for DAG-1

The explosive source for DAG-1 was nitromethane initiated by a small plastic-bonded explosive (PBX) charge, and had a TNT equivalent yield of 0.908 metric tons (2,002 lbs). The canister was

1.173 m (3.848 ft) in length and 1.048 m (3.438 ft) in diameter, for a length-to-diameter ratio of 1.120. After the canister was positioned at the top of the source hole, it was loaded with nitromethane prior to being lowered down the hole into position. The canister was installed in the source hole so that the center of the explosive charge was at the depth of 385.0 m (1,263.2 ft) below ground surface.

Prior to stemming operations, fill was tagged in the source hole at 395.3 m (1,297 ft) below ground surface. A lift of ⅜-in. gravel was placed to the depth of 388.0 m (1,273 ft) below ground surface on top of the fill prior to installation of the canister. To fully confine the explosive source, the canister was surrounded by Overton sand up to the depth of 379.9 m (1,246.5 ft) below ground surface. Three alternating layers of ⅜-in. gravel and 40/100 sand (concrete sand) were placed above the sand to the depth of 313.9 m (1,030 ft) below ground surface. A 3.4-m (11-ft) thick grout plug was placed above the last layer of concrete sand to a depth of 310.6 m (1,019 ft) below ground surface. Lastly, a 2.7-m (9-ft) thick lift of 20/40 sand was placed on top of the grout plug to the depth of 307.8 m (1,010 ft) below ground surface (Figure 4).

The DAG-1 test was conducted on July 20, 2018 (day 201), at 16:51:52.67838 Coordinated Universal Time (UTC). The location was 37.114644234, -116.06926431, at a centroid depth of 385.0 m (1,263.2 ft). The explosion was well confined, with no prompt (<1 second) ejecta or gas release.

4.2 Explosive Source and Detonation for DAG-2

The explosive source for DAG-2 was nitromethane initiated by a small PBX charge, and had a TNT equivalent yield of 50.997 metric tons (112,429 lbs). The canister was 11.969 m (39.268 ft) in length and 2.115 m (6.939 ft) in diameter, for a length-to-diameter ratio of 5.66. After the canister was positioned at the top of the source hole, it was loaded with nitromethane prior to being lowered down the hole into position. The canister was installed in the source hole so that the center of the explosive charge was at the depth of 299.8 m (983.6 ft) below ground surface.

Prior to emplacement of the canister, 20/40 sand was placed to the depth of 306.6 m (1,006 ft) below ground surface on top of the DAG-1 stemming and cable debris. To fully confine the explosive source, the canister was surrounded by Overton sand up to the depth of 289.7 m (950.5 ft) below ground surface. Three alternating layers of ⅜-in. gravel and 40/100 sand (concrete sand) were placed above the Overton sand to the depth of 160.0 m (525 ft) below ground surface. A 5.2-m (17-ft) thick grout plug was placed above the last layer of concrete sand to a depth of 154.8 m (508 ft) below ground surface. Lastly, a 3.0-m (10-ft) thick lift of 20/40 sand was placed on top of the grout plug to the depth of 151.8 m (498 ft) below ground surface (Figure 5).

The DAG-2 test was conducted on December 19, 2018 (day 353), at 18:45:56.92115 UTC. The location was 37.114644234, -116.06926431, at a centroid depth of 299.8 m (983.6 ft). The explosion was well confined, with no prompt (<1 second) ejecta or gas release. DAG-2 registered as a 2.33 magnitude earthquake according to the Nevada Seismological Laboratory (http://www.seismo.unr.edu/Events/main.php?evid=670843). Seismic activity continued for about two days after detonation.

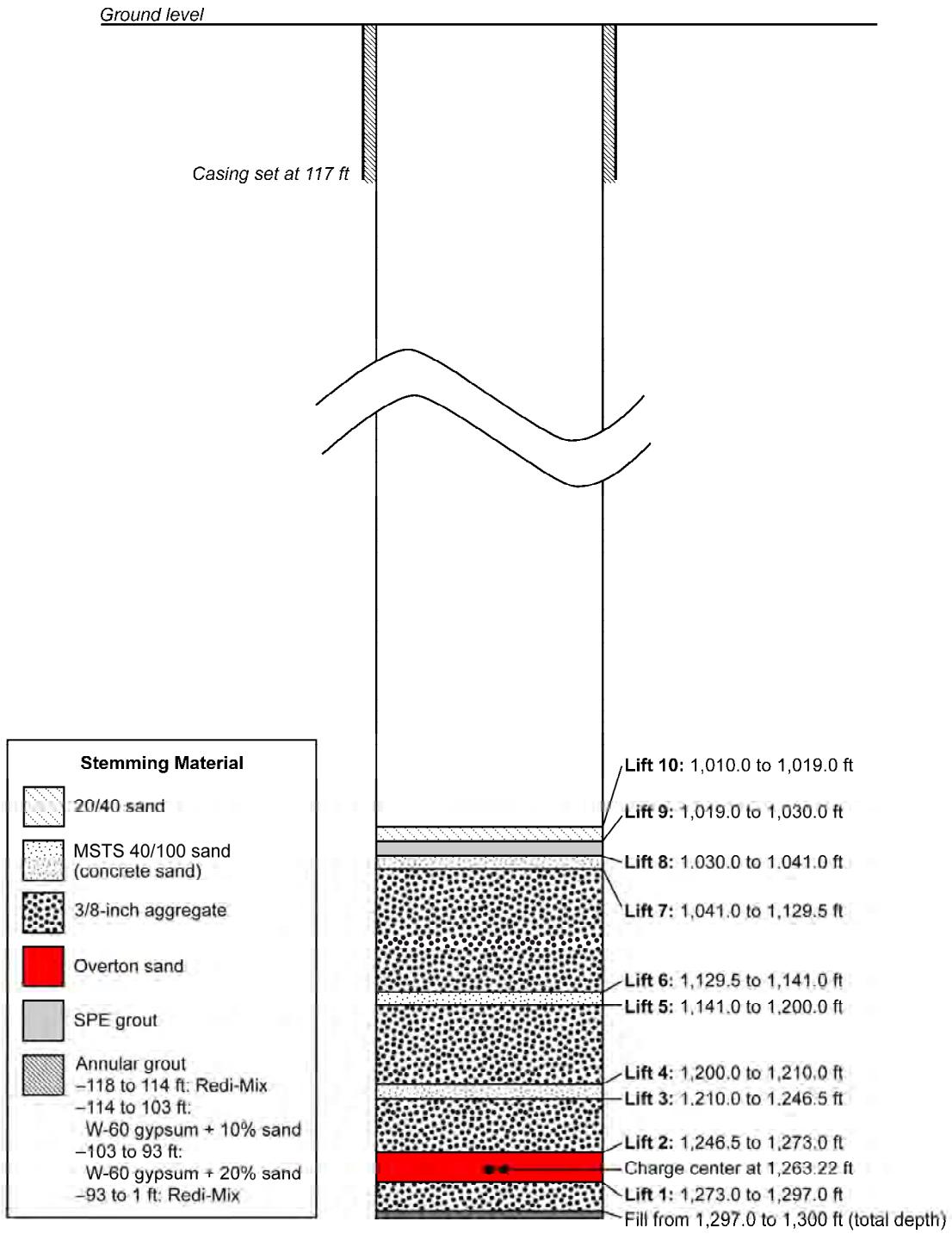

Figure 4
Schematic Drawing Showing Placement of Explosives and Stemming in DAG-1 Source Hole

.

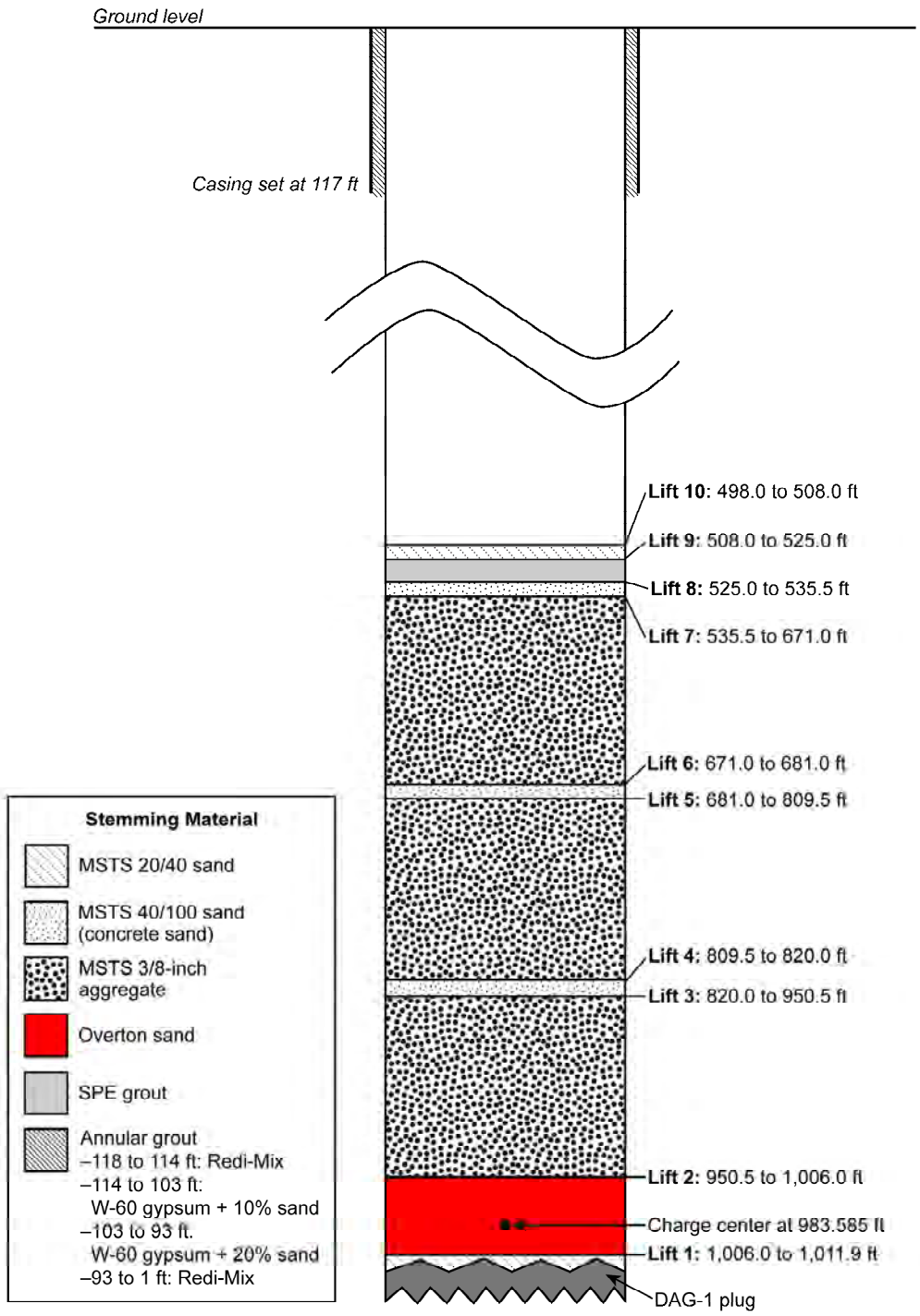

Figure 5
Schematic Drawing Showing Placement of Explosives and Stemming in DAG-2 Source Hole

4.3 Explosive Source and Detonation for DAG-3

The explosive source for DAG-3 was nitromethane initiated by a small PBX charge, and had a TNT equivalent yield of 0.908 metric tons (2,002 lbs). The canister was 1.173 m (3.848 ft) in length and 1.048 m (3.438 ft) in diameter, for a length-to-diameter ratio of 1.120. After the canister was positioned at the top of the source hole, it was loaded with nitromethane prior to being lowered down the hole into position. The canister was installed in the source hole so that the center of the explosive charge was at the depth of 149.9 m (492.0 ft) below ground surface.

Prior to emplacement of the canister, 20/40 sand was placed to the depth of 150.9 m (495 ft) below ground surface on top of the DAG-2 stemming and cable debris. To fully confine the explosive source, the canister was surrounded by Overton sand up to the depth of 146.9 m (482 ft) below ground surface. An 83.5-m (274-ft) thick layer of ⅜-in. gravel was placed above the Overton sand followed by a 3.0-m (10-ft) thick layer of 40/100 sand (concrete sand). A 3.4-m (11-ft) thick grout plug was placed above the concrete sand to a depth of 57.0 m (187 ft) below ground surface. Lastly, a 2.4-m (8-ft) thick lift of 20/40 sand was placed on top of the grout plug to the depth of 54.6 m (179 ft) below ground surface (Figure 6).

The DAG-3 test was conducted on April 27, 2019 (day 117), at 15:49:01.84183 UTC. The location was 37.114644234, -116.06926431, at a centroid depth of 149.9 m (492.0 ft). The explosion was well confined, with no prompt (<1 second) ejecta or gas release. DAG-3 registered as a 0.40 magnitude earthquake according to the Nevada Seismological Laboratory (http://www.seismo.unr.edu/Events/main.php?evid=683377).

4.4 Explosive Source and Detonation for DAG-4

The explosive source for DAG-4 was nitromethane initiated by a small PBX charge, and had a TNT equivalent yield of 10.357 metric tons (22,833 lbs). The canister was 3.080 m (10.105 ft) in length and 2.134 m (7.001 ft) in diameter, for a length-to-diameter ratio of 1.444. After the canister was positioned at the top of the source hole, it was loaded with nitromethane prior to being lowered down the hole into position. The canister was installed in the source hole so that the center of the explosive charge was at the depth of 51.6 m (169.3 ft) below ground surface.

Prior to emplacement of the canister, a 1.1-m (3.5-ft) lift of 20/40 sand was placed on top of the DAG-3 stemming and cable debris. To fully confine the explosive source, the canister was surrounded by Overton sand up to the depth of 46.2 m (151.5 ft) below ground surface. A 15.8-m (52-ft) thick layer of ⅜-in. gravel was placed above the Overton sand followed by a 25.5-m (83.5-ft) thick layer of 40/100 sand (concrete sand). The remainder of the hole was grouted to the surface (Figure 7).

The DAG-4 test was conducted on June 22, 2019 (day 173), at 21:06:19.87632 UTC. The location was 37.114644234, -116.06926431, at a centroid depth of 51.6 m (169.3 ft). The explosion was well confined, with no prompt (<1 second) ejecta or gas release. DAG-4 registered as a 1.96 magnitude (ML) earthquake according to the Nevada Seismological Laboratory (http://www.seismo.unr.edu/Events/main.php?evid=688352).

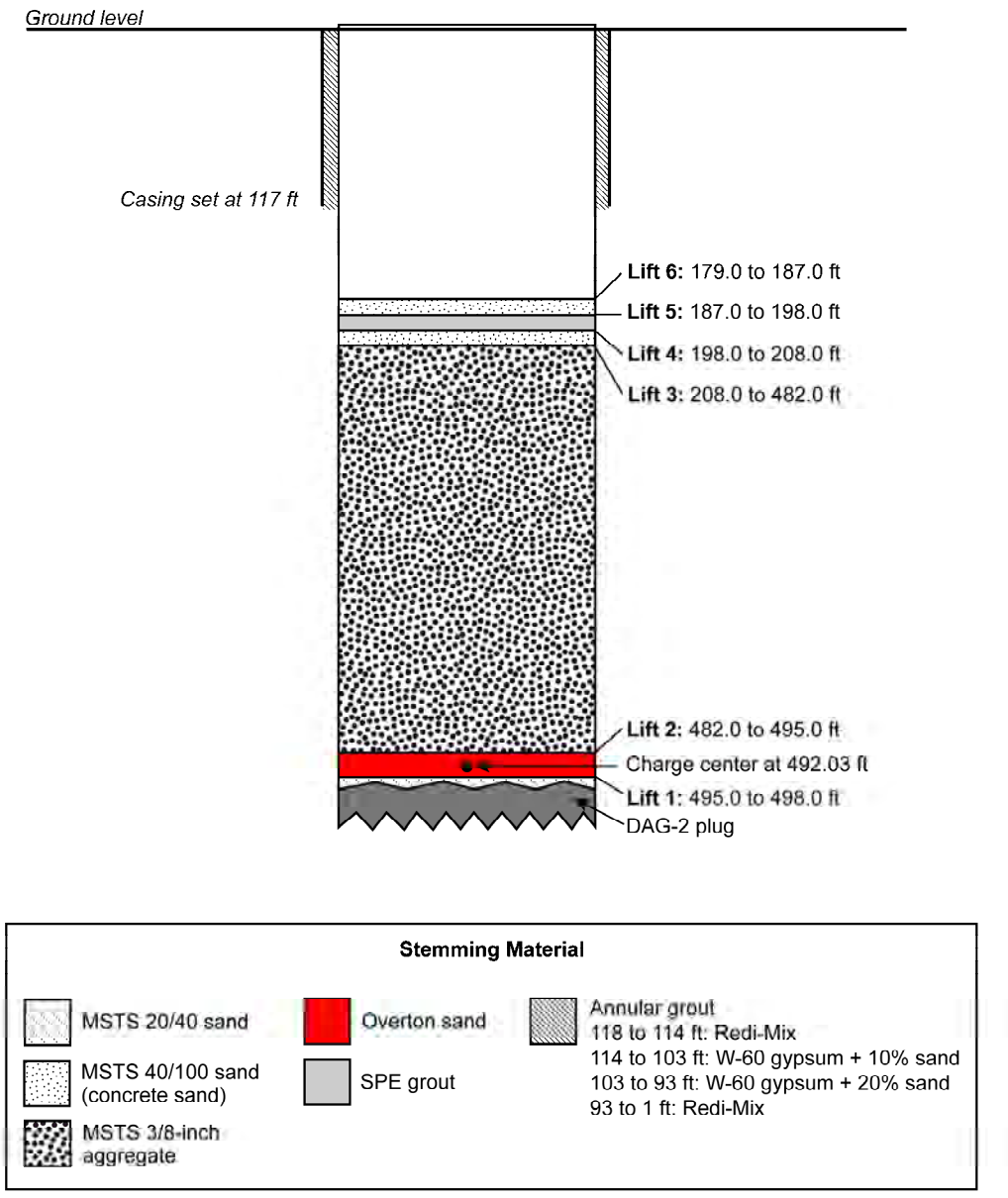

Figure 6
Schematic Drawing Showing Placement of Explosives and Stemming in DAG-3 Source Hole

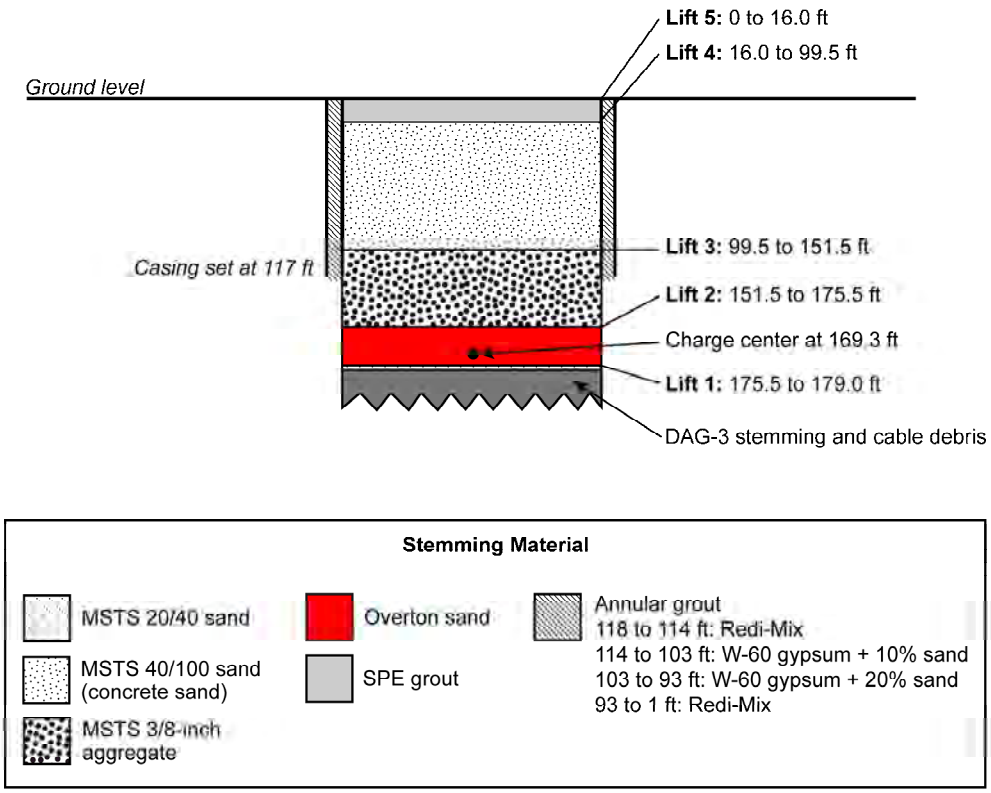

Figure 7
Schematic Drawing Showing Placement of Explosives and Stemming in DAG-4 Source Hole

4.5 Detonation Diagnostics (Corrtex)

Corrtex (COntinuous Reflectometry for Radius vs. Time Experiment) utilized time domain reflectometry, pulsed at 100 kilohertz, to actively measure the lengths of cables that were installed on each DAG experimental package. Each of the four DAG experiments included six Corrtex cables: two inside the package, installed along the pipes that secured the initiation fixture at the device center, and four outside the package, installed in angle brackets along the cannister's exterior wall. Installation in DAG-1 and DAG-2 are shown in Figures 8 and 9, respectively; installation in DAG-3 and DAG-4 was very similar. Because the Corrtex cables proceed up-hole from the device, and because the device is initiated at its center, Corrtex data provided a record of detonation for the top half of each experiment, with cable lengths measured every 10 microseconds to record the progress of the detonation wave. In addition, Corrtex cable lengths were recorded through the initial period of grout/rock crush above the DAG cannister. In each experiment, Corrtex successfully recorded cable length change throughout the detonation of the nitromethane. No issues were encountered in the fielding of this diagnostic, or in the reduction of data from the four DAG experiments.

For each of the four DAG tests, data comprise cable length measurement as a function of time for each of the six cables. The data record for each cable is given as two columns: one for time

Figure 8
DAG-1 Corrtex Installation
On the left photo, a red oval designates one of four external channels into which Corrtex cables were inserted. Cables were truncated at the first sign of detonation along the cannister wall. The photo on the right is the initiation package inserted into the DAG-1 cannister. Corrtex was installed within two of the four pipes.

Figure 9
DAG-2 Corrtex Installation
As in Figure 8, red ovals on the left photo designate start and end point for one of four external conduits used for Corrtex cables. The photo on the right shows the insertion of the initiator package into the DAG-2 cannister. As for DAG-1, Corrtex cables were installed in two of the four pipes.

(measured in seconds), and one for the net cable length change (measured in meters) since the start of each test. Corrtex cables 1 and 2 were truncated by the nitromethane detonation directly up the axis of the test canister from the initiation unit, and hence are a direct measurement of the detonation velocity. Corrtex cables 3 through 6 were installed in angle iron channels on the outside of the device, and are placed symmetrically; data from these channels show truncation of the cables at the device centerline (adjacent the initiator), followed by rapid but decelerating cable truncation speed as the detonation wave propagates up the device, with an asymptotic approach of truncation speeds to the detonation velocity. Because of the similarity between cable installation geometries (1 and 2 vs. 3 through 6), data for cables 1 and 2 are identical, and data for cables 3 through 6 are identical. This was the expectation due to the design, and confirmed that all four DAG experiments were perfectly symmetric tests. Data from all cables deviated significantly after the nitromethane was fully consumed. There was speculation that cable length changes beyond this time indicated the speed at which rock was crushed by the expanding shockwave surrounding the hole in which the devices were buried. Plots of the data from each experiment are presented in Figures 10 through 13.

5 Near-Field Instrumentation

Near-field instrumentation (defined as less than 200 m from the source) for the DAG experiments included accelerometers installed in boreholes and on the surface, as described in this section.

5.1 Borehole Accelerometers

As described in Section 3.1.2, twelve boreholes were drilled to accommodate installation of near-field instrumentation packages. Each package consisted of a 3C accelerometer, with triaxial sets mounted 120 degrees apart on the same radius. All ranged a minimum of three times the maximum predicted acceleration. They had a minimum 5,000 g shock survival rating. The Z axis was oriented upward, and the X and Y axes are orthogonal to Z.

As described in Section 3.1.2 and shown in Figure 3, three lines of holes were drilled at distances of 10, 20, 40, and 80 m from the source holes. Figure 14 is a schematic illustration of the positions of the accelerometer packages in each hole relative to the DAG experiment locations along one line.

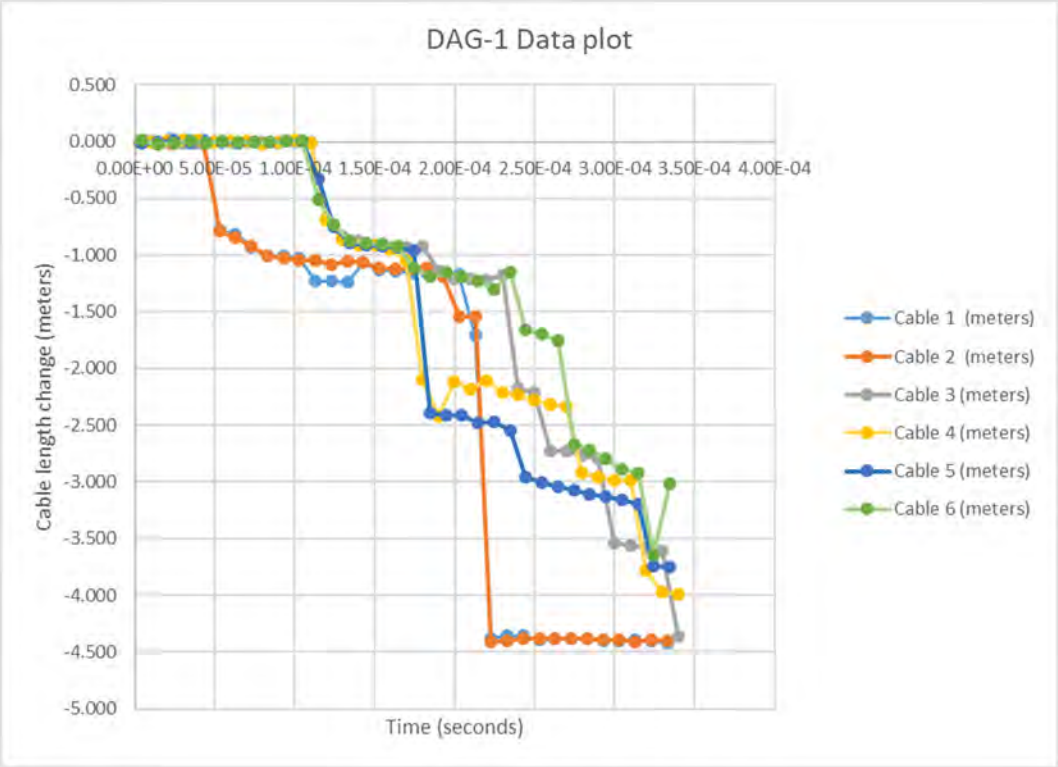

Figure 10
Plot for DAG-1 Corrtex Data

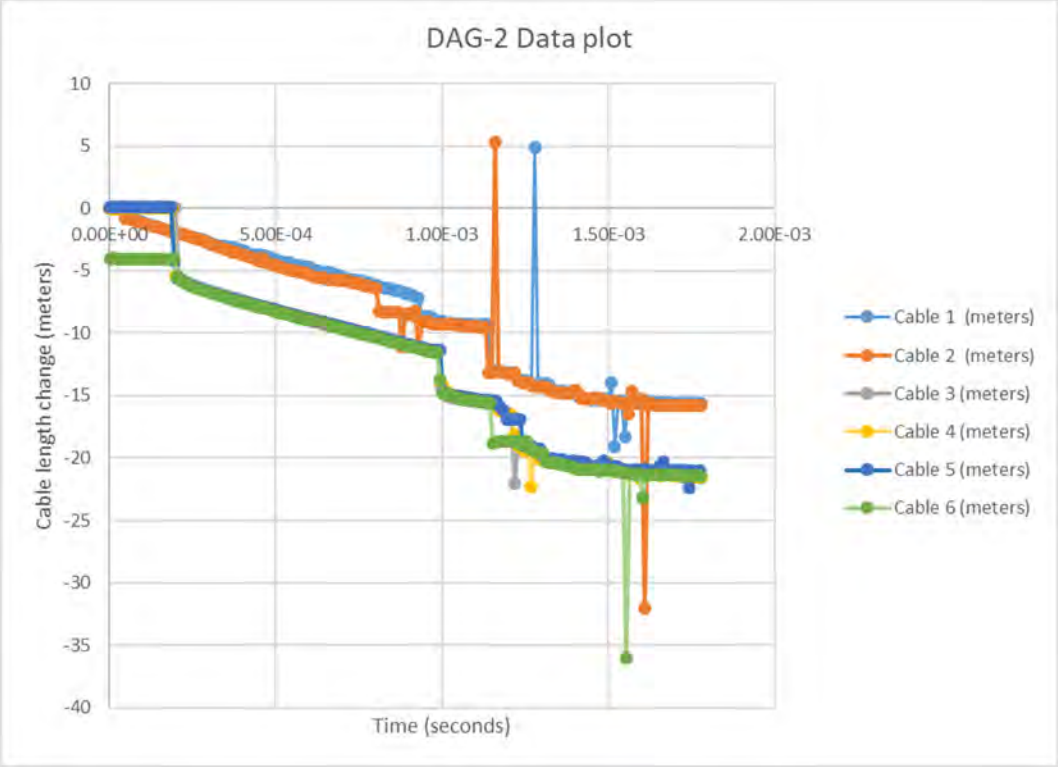

Figure 11
Plot for DAG-2 Corrtex Data

Figure 12
Plot for DAG-3 Corrtex Data

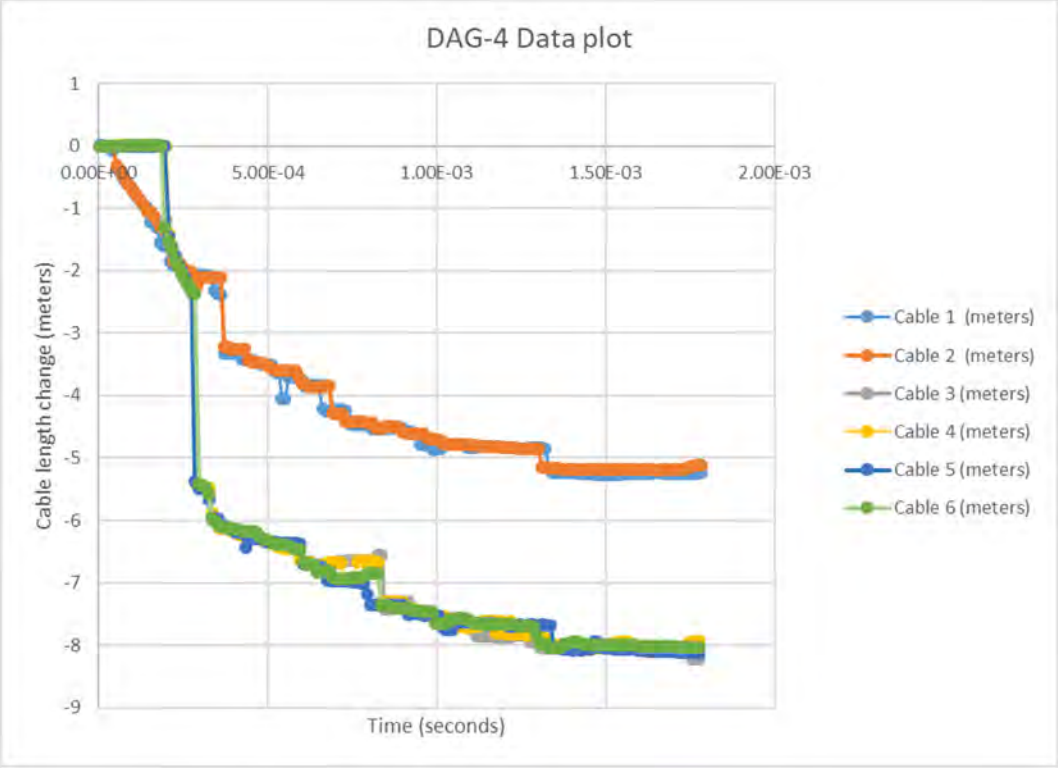

Figure 13
Plot for DAG-4 Corrtex Data

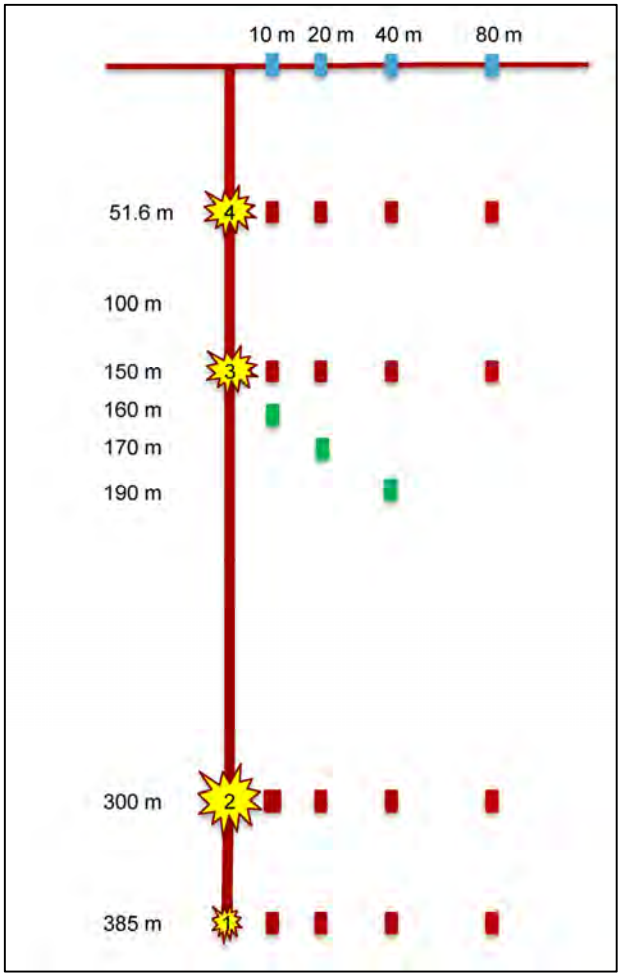

This diagram illustrates, in side view, the arrangement of the borehole accelerometer packages in each of three lines of holes drilled for the DAG tests. The depths of the four DAG tests are indicated by the yellow icons. Four holes were drilled along each line at 10, 20, 40, and 80 m from the DAG source hole. The lateral distance of each instrument hole is indicated in blue across the top. The red pods indicate sensors in place for all four tests. The green sensors were added after the DAG-2 test to record DAG-3 and DAG-4.

Figure 14
Diagram Showing Typical Near-Field Borehole Accelerometer Package Arrangement along a Line of Instrument Holes for All DAG Tests

5.2 Near-Field Surface Accelerometers

A near-field surface accelerometer array was installed within 200 m of the U-2ez source hole to capture the extent, if any, of surface spall and supplement the near-field high-shock accelerometers in satellite boreholes. At the surface, accelerometers were installed in six lines radiating out from the surface location of the DAG test ("surface ground zero," or SGZ) spaced at 60-degree increments azimuthally. The number and spacing of deployed surface accelerometers varied among the DAG tests (Figures 15 through 17). For DAG-1, 24 accelerometers were spaced in 20-m increments. For DAG-2 and DAG-3, 42 accelerometers were spaced in 10-m increments. For DAG-4, the spacing of 48 accelerometers varied from 10 to 70 m. For all of the tests, some accelerometers contained single channel vertical components (channel FNZ) and others included 3C sensors (channels FNZ, FNR, and FNT) with horizontals oriented in the radial and transverse directions.

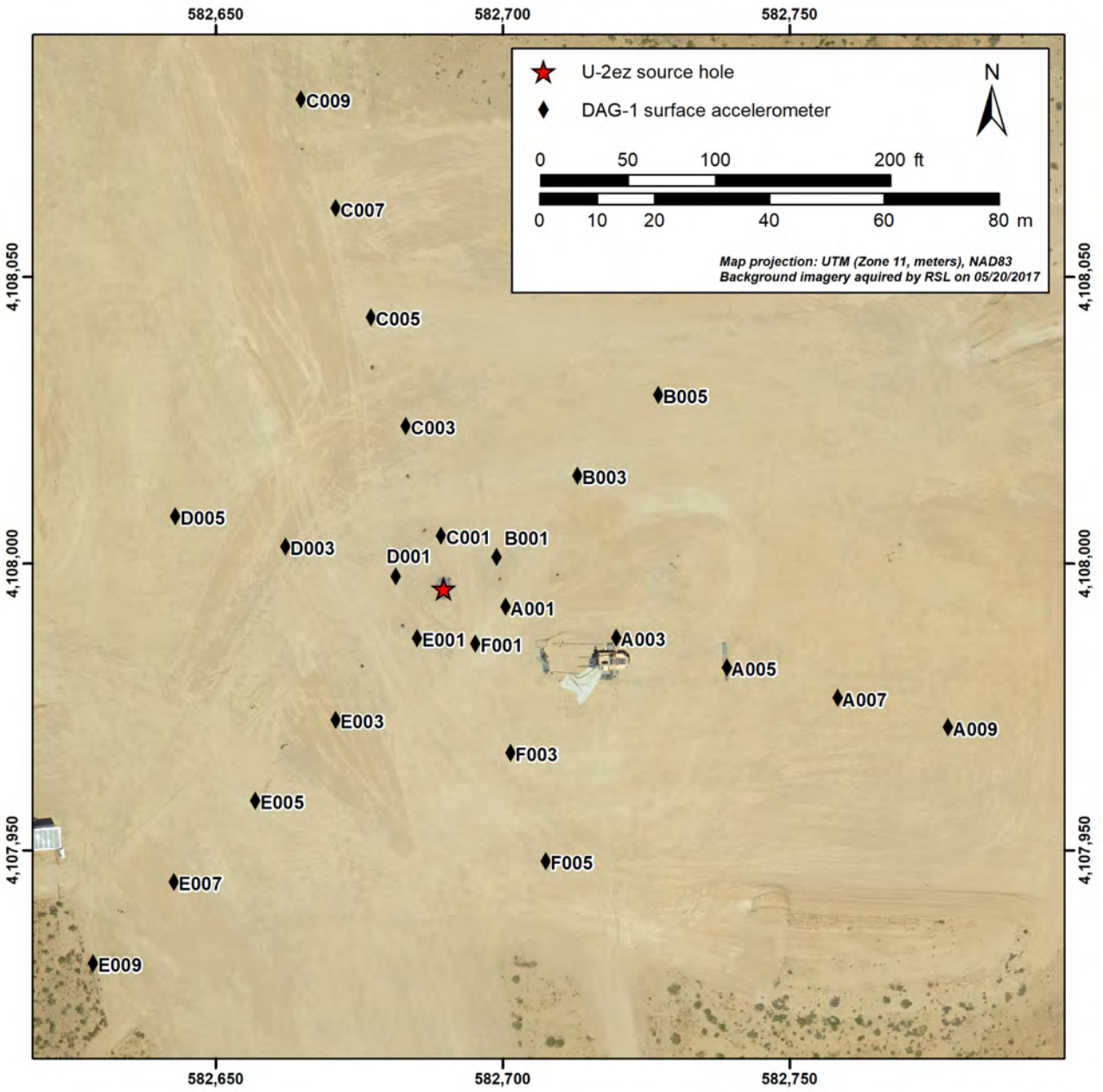

Figure 15
Map Showing Locations of the Near-Field Surface Accelerometers Deployed During DAG-1

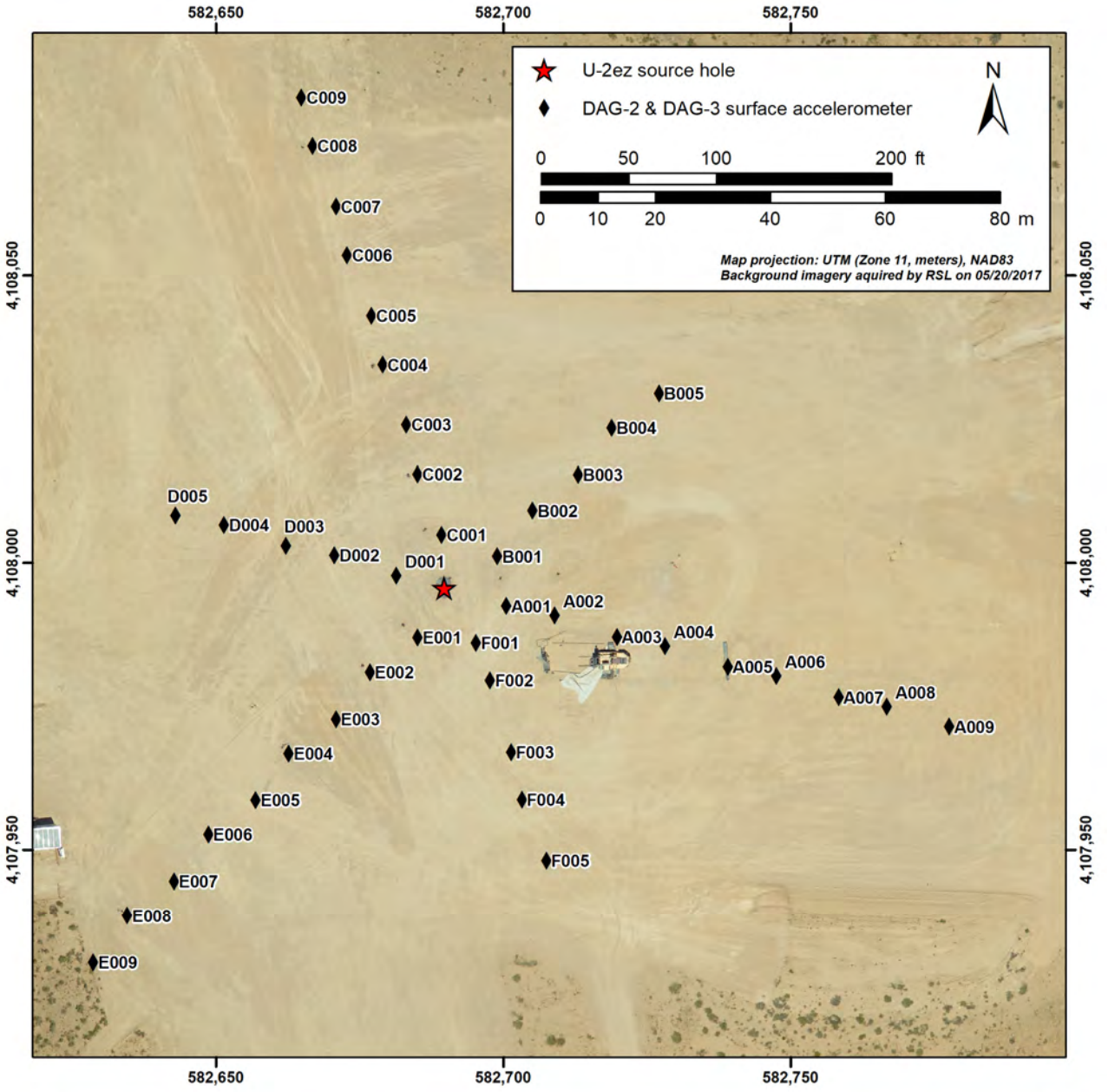

Figure 16
Map Showing Locations of the Near-Field Surface Accelerometers Deployed during DAG-2 and DAG-3

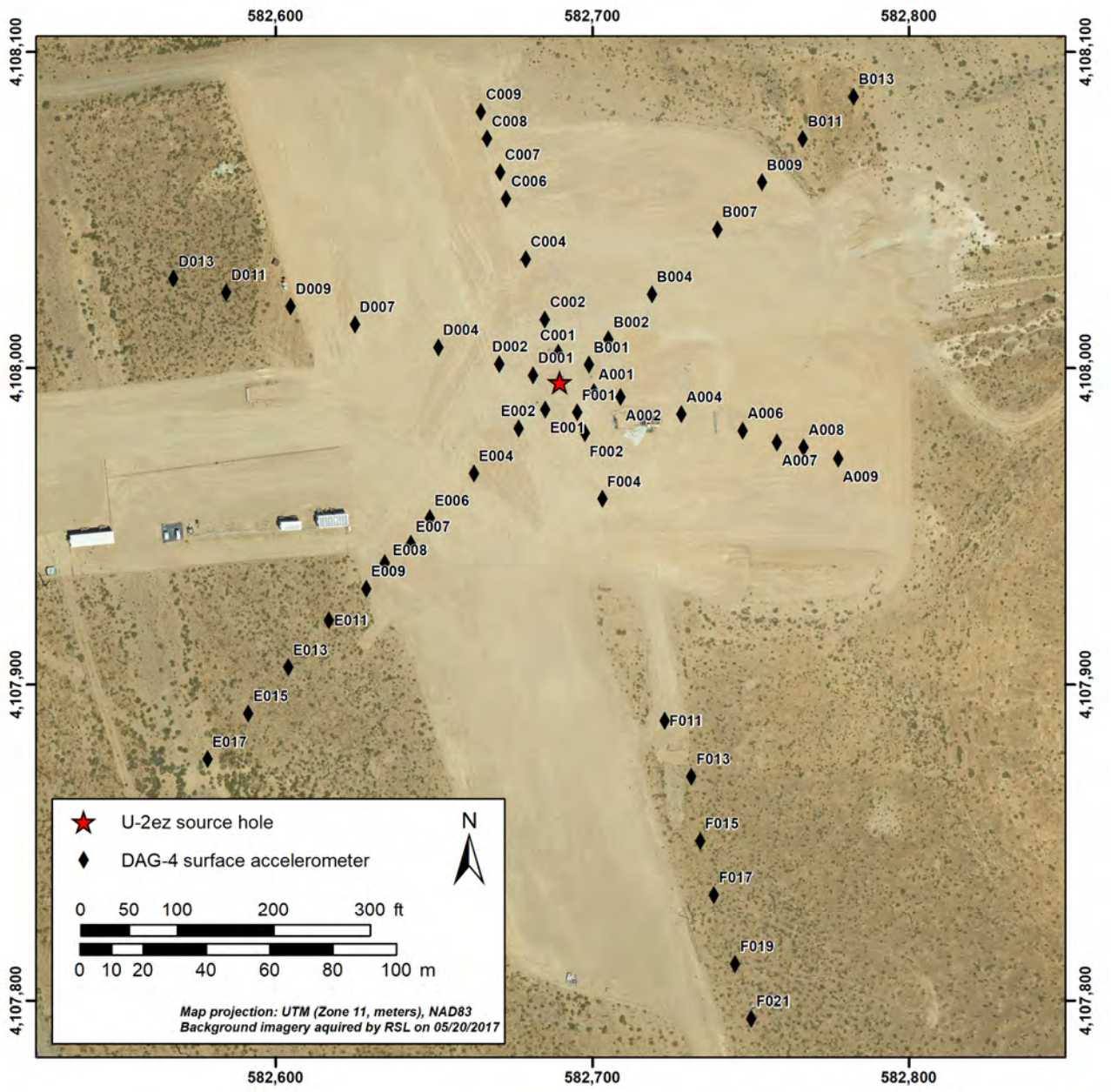

Figure 17
Map Showing Locations of the Near-Field Surface Accelerometers Deployed During DAG-4

6 Far-Field Instrumentation

Three primary types of far-field sensors (seismic, infrasound, and weather) were deployed for the DAG tests, as described in the following sections. The waveform sensor data in this data release used the Federation of Digital Seismograph Networks (FDSN.org) network code SN (Southern Great Basin Network).

The far-field surface seismic range is differentiated from near-field surface and borehole seismic sensors by distance (i.e., 200 m from the source hole), which was approximately four times beyond the predicted elastic radii of the largest DAG experiment (<50 m). In the near field, high-shock accelerometers were required inside the zone of nonlinear hydrodynamic deformation, while the far field is considered a zone of linear-elastic deformation.

6.1 Surface Seismic Instrumentation

To characterize the far-field seismic wavefield (defined as 200 m or more from the source), a number of different instrument arrays were deployed to distances as great as 400 km. The primary set of far-field seismic data collected came from geophones and accelerometers in place for all four of the DAG tests conducted. An additional set of data was collected from a grid of 496 closely spaced geophones ("Large N") placed within 200 to 2,500 m of SGZ. The following sections provide information about the various seismic arrays.

6.1.1 Geophones, Accelerometers, and Broadbands

The surface seismic far-field instrumentation for the DAG experiments consisted of 3C geophones, accelerometers, and broadband sensors deployed in various geometries around the U-2ez source hole (Figure 18). Most of these sensors were buried in shallow postholes to improve coupling in the alluvium. The data was recorded using 6-channel RefTek digitizers powered by batteries trickle charged from solar panels. The data were then telemetered in real time to the Nevada Seismological Laboratory at UNR.

6.1.1.1 Geophones

The 3C Geospace GS11D surface geophone geometries included lines, rings, and arrays. The geophone lines consisted of 16 geophones (station codes GL00–GL15) arranged in north-south and east-west lines, with four geophones placed between 200 and 500 m in 100 m increments extending linearly out from SGZ (Figure 19). The geophone rings consisted of 42 3C Geospace GS11D geophones deployed around SGZ (Figures 18 and 19). The naming convention for the rings included two numbers, the distance from SGZ (radii of 0.5 km, 1.5 km, and 2.0 km as G5, G15, and G20) followed by 'M', and a sequential number from 0 to 9 or A, clockwise from north. Eight or nine geophones were arranged in 3 rings with radii of 0.5 km (station codes G5M00–G5M09), 1.5 km (station codes G15M0–G15M7), and 2 km (station codes G20M0–G20MA). The geophones in each ring were separated by approximately 45-degree increments in azimuth around SGZ.

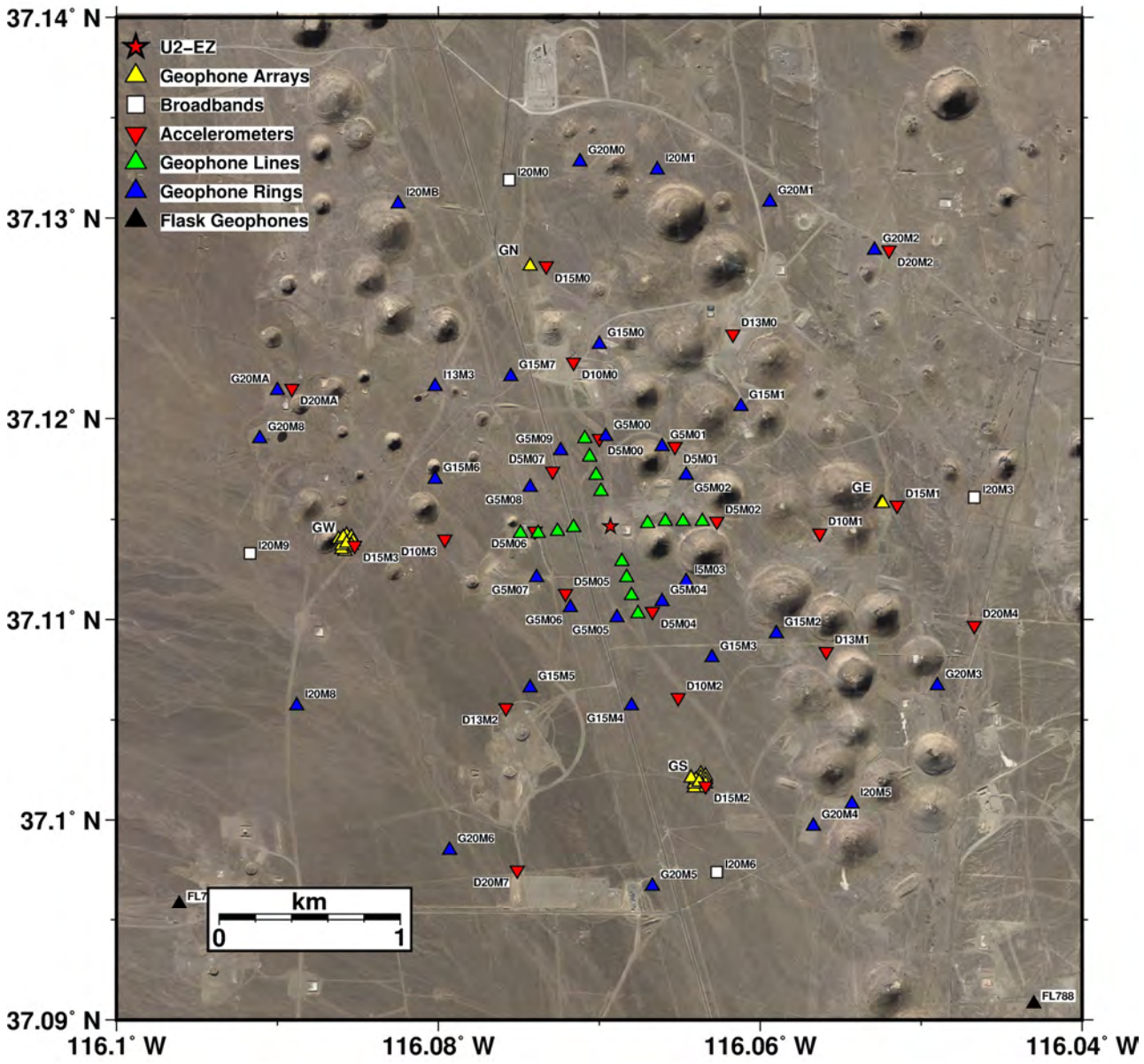

Figure 18
Map Showing Locations of Surface Seismic Sensors in the Far-Field for the DAG Experiments
See expanded view of the four geophone small aperture arrays (yellow triangles) on Figure 20.

Exceptions to the naming conventions for the geophone rings occurred at several sites to note the inclusion of an infrasound sensor (e.g., station code I20M1). There were some gaps in sensor surface coverage due to neighboring collapse craters created by historical underground nuclear explosions. The horizontal geophone channels (DLR and DLT) were oriented away from the direction of the source hole in radial direction, transverse was perpendicular clockwise from radial, and vertical channel DLZ is oriented positive downward (see Subsections 6.1.1.1.1 and 6.1.1.1.2 for polarity standards and orientation corrections).

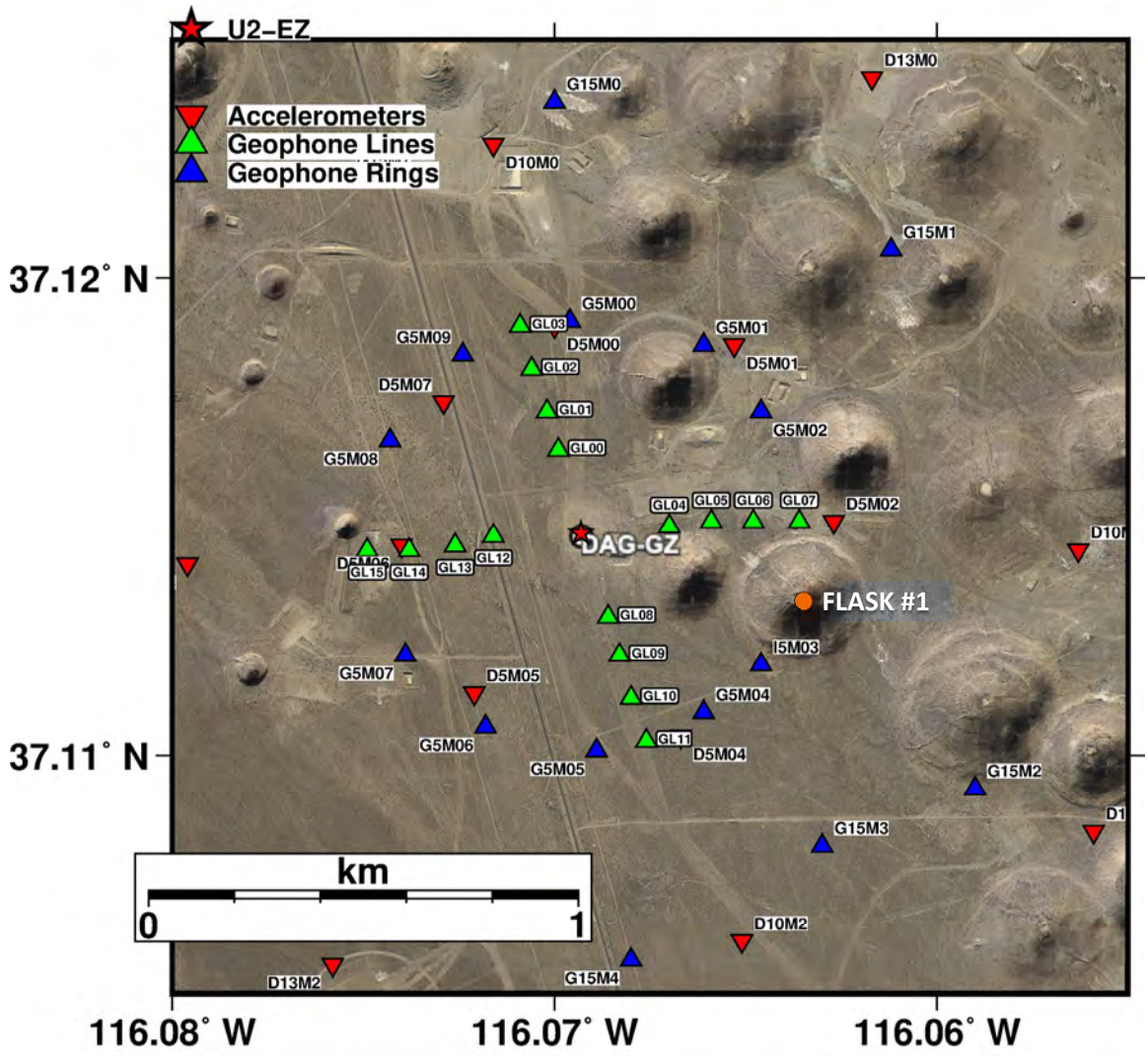

Figure 19
Map Showing Locations of Surface Seismic Sensors Placed within Approximately 1 Kilometer of U-2ez Including Geophone Lines

Four geophone arrays were located approximately 1.5 km from SGZ in two types of small-aperture array designs (Figures 18 and 20). Gradiometer arrays were located 1.5 km north (GN) and 1.5 km east (GE) of SGZ (Figure 18). Both arrays had an aperture length of 4 m and consisted of 13 geophones (station codes GN01–GN13) arranged in a circle with a radius of 2 m about a center geophone (GN14). Array GW was located 1.5 km west and array GS was located 1.5 km south of SGZ (Figure 18 and 20). Both of these arrays had apertures of approximately 100 m and also consisted of 14 total geophones (station codes GW01–GW14) but with different designs (Figure 20). The horizontal geophone channels (DLN and DLE) were oriented in north-south and east-west configurations for array processing (see Subsections 6.1.1.1.1 and 6.1.1.1.2 for polarity standards and orientation corrections).

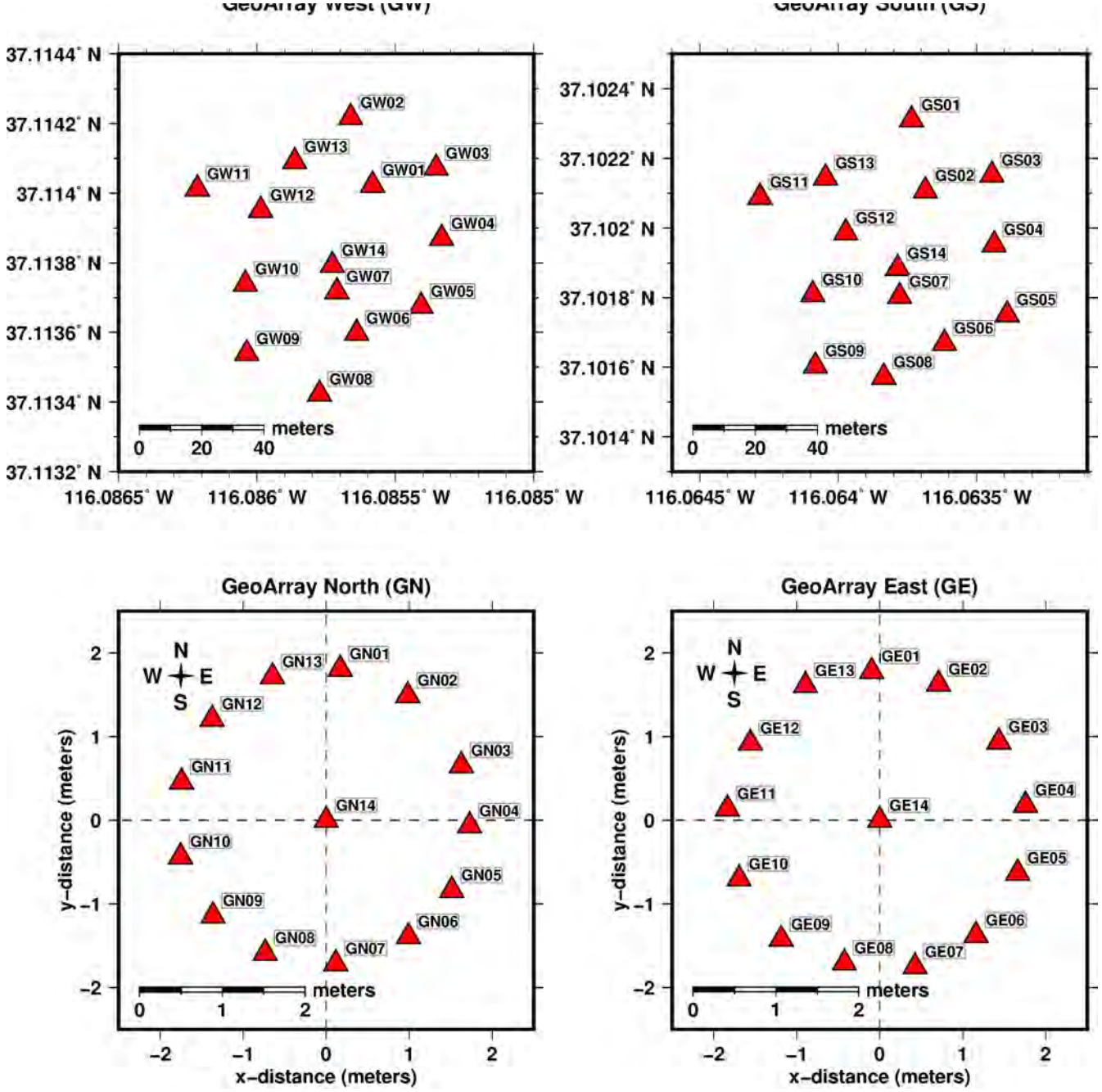

Figure 20
Maps Showing Locations of the Four Geophone Small Aperture Arrays
See Figure 18 for locations in relation to SGZ.

Twelve geophones (station codes FL781 and FL785–FL795) were deployed to reoccupy the sites instrumented for the FLASK underground nuclear explosive test conducted on May 26, 1970 (U.S. Department of Energy 2015). The FLASK #1 crater is approximately 600 m east-southeast from SGZ (Figure 19). The reoccupied instrumentation sites ranged between 2.5 and 3.5 km from U-2ez, forming a circle around SGZ (Figure 21). The horizontal geophone channels (DLN and DLE) were oriented in south-to-north and west-to-east configurations for array processing (see Subsections 6.1.1.1.1 and 6.1.1.1.2 for polarity standards and orientation corrections).

All geophone channels recorded continuously at a sampling rate of 500 samples per second (sps) (Nyquist frequency of 250 hertz [Hz]. The geophones have a natural frequency of 4.5 Hz. All the RefTek 130 digitizer gains were set to full amplification factor of 32. The gain was reduced to an amplification of one within a day before the experiments and subsequently increased back to 32 within a few days in order to record the cable-cutter shots. The higher gain setting between experiment times allowed for the recording of background noise and lower gain setting allowed for on-scale recording of the explosions with minimal clipping. The exception was with DAG-1, where the digitizer gains were not changed from 32, since clipping was not expected due to the smaller size and greater depth of this test.

6.1.1.1.1 Geophone Polarity Standards

It is important to note that data polarity standards for geophones and seismometers differ. Geophones produce negative voltages for upward ground motions, while the broadband seismometers and accelerometers produce positive voltages for upward ground motion. This polarity standard is extended to all three components in the case of the 3C geophones. The right-hand-rule, a common mnemonic for understanding orientation of axes in 3D, was used with the vertical axes pointing into the Earth. Orientations were set in the field visually and later verified by compass. Timings were established by global positioning system (GPS) receivers at each digitizer.

6.1.1.1.2 Geophone Sensor Orientation Corrections

There is an error in the metadata for all geophone channels (DL) which is not to be confused with the geophone polarity standard. This error was corrected in this data release. The vertical and horizontal orientations required either a ‘-1’ multiplier or subtraction of 180 degrees with 360-degree modulo operation (“wrap-around 360 function”). The Python code snippet in Figure 22 demonstrates the correction of dip and azimuth in files formatted according to the Standard for the Exchange of Earthquake Data (SEED) formatted files.

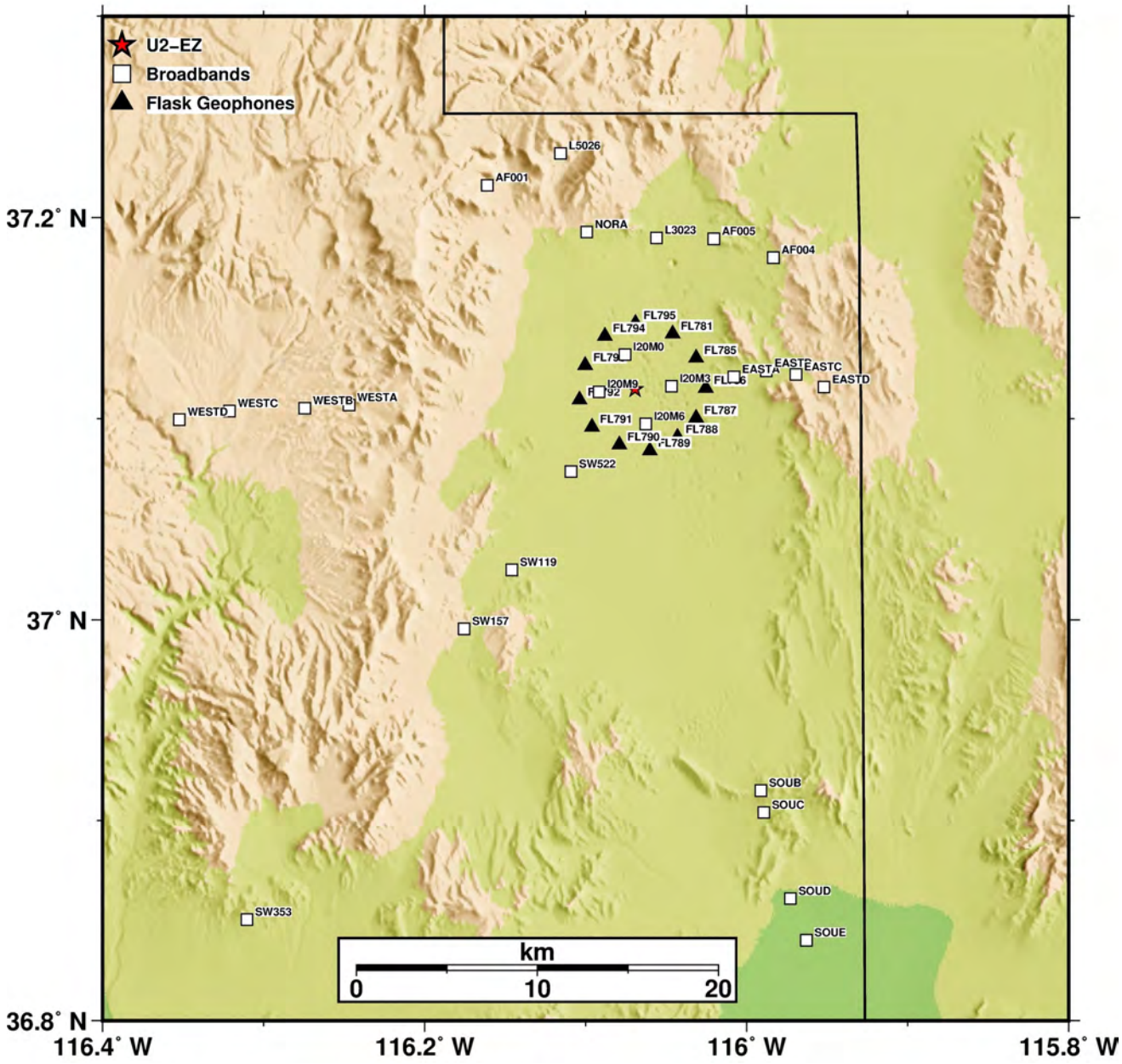

Figure 21
Map Showing Location of the Flask Geophone Array and Broadband Seismic Sensors

```
from obspy.io.xseed import Parser
p = Parser( "dag_dataless_seed_fullres_v2_0" )
blk = p.blockettes
for i in range( 0, 4528, 1 ):
        chan = blk[52][i].channel_identifier
        if chan == "DLZ":
                dip0 = blk[52][i].dip
                blk[52][i].dip = -1 * dip0
        if chan == "DLN" or chan == "DLE" or chan == "DLR" or chan == "DLT":
                az0 = wrap_around360( blk[52][i].azimuth - 180.0 )
                blk[52][i].azimuth = az0
p.write_seed( "test.seed" )
```

Figure 22
Snippet of Python Code Demonstrating the Correction of Dip and Azimuth in SEED-Formatted Files

In addition to the differing polarity conventions between sensor types, there are also differences in the definition of orientation stored in the metadata formats. The sensors' vertical orientation angle is recorded in the variable CMPINC, DIP, or VANG in SAC headers, SEED channel blockettes, and CSS sitechan formats respectively. For the SAC and CSS formats, the incident angle of 0 is vertical upwards and 180 downwards; however, the SEED convention is +90 upward and -90 downward. The sensors horizontal orientation angle (degrees clockwise from north) is recorded in the variable CMPAZ, AZI, or HANG in SAC, SEED, and CSS formats respectively. There are no differences between the formats with the horizontal orientation angle. Therefore, regardless of the formatting, the logic applied to the SEED volume, can instead be applied to CSS or SAC metadata.

Users can test and verify these corrections by FDSN SEED volume reader (rdseed) application and output to SAC files using the dash 'z' option to apply polarity reversal corrections to the data (Figure 23). The data can also be extracted without the dash 'z' option.

```
rdseed -f data.miniseed -d -o 1 -g dataless.seed -z 1

The following options are (see manual for full list):
-f seed or miniseed volume file name
-d dump the data records
-o data output format (SAC=1)
-g specify alternative response file (i.e. dataless SEED for miniseed)
-z check and correct reversals (0=no 1=dip, azimuth 2=gain 3=both)
```

Figure 23
Information about the FDSN SEED Volume Reader

Both extraction methods can be tested with explosion data, given the expectation that first motion polarities are positive on the vertical component oriented upwards and positive on horizontal components oriented outwards. Comparisons can also be performed with nearby co-located

accelerometers where available. When using rdseed to extract SAC files with the corrected metadata, the dash 'z' option results in CMPINC=0 (oriented upwards) for the DLZ vertical-component and a positive first-motion polarity consistent with explosion first-motion expectation. The same for the radial component, CMPAZ which now points outward consistent with the positive radial first-motion polarity. Without the dash 'z' option, the vertical orientation is not changed (i.e., CMPINC=180) and the DLZ vertical-component is left in the geophone standard with negative first-motion polarity. The same can also be applied to the geophone arrays and FLASK arrays recorded using the DLN and DLE components and were verified using the 'rotate' command in SAC.

6.1.1.2 Accelerometers

The 22 accelerometers deployed around SGZ were arranged with a similar naming convention as the geophone rings (Figures 18 and 19). The Kinemetrics EpiSensor or EpiSensor2 force balance accelerometers were combined with RefTek 130S data acquisition systems. The naming convention for the rings included two numbers, the radii from SGZ (0.5km, 1.3km, 1.5km, and 2.0km as D5, D13, D15, and D20) followed by 'M' and a sequential number from 0 to 9 or A, clockwise from north. There were some gaps in sensor surface coverage due neighboring collapse craters created by previous historical underground nuclear explosions. The horizontal geophone channels (CNR and CNT) were oriented toward the source hole in radial and transverse configurations, and vertical channel CNZ is oriented positive upward. Two accelerometers (U1AS and U1AU) located in Area 1 of the NNSS had horizontal components oriented in north-south and east-west configurations (CNN and CNE). The accelerometer sampling rates were 500 sps and Nyquist frequency 250 Hz. The exception was with stations U1AS and U1AU set to a rate of 250 sps.

6.1.1.3 Broadbands

The 26 broadband sensors were deployed around SGZ and within the NNSS boundary (Figure 21). Instrumentation included Nanometrics Trillium 120 Compact sensors and RefTek 130S or Kinemetrics Quanterra Q330 data acquisition systems. Four of these broadbands (I20M0, I20M3, I20M6, and I20M9) were within a 2-km geophone ring around SGZ. Some of the broadband sites from SPE Phase I remained in place for DAG, including three instruments place by AFTAC (AF001, AF004, and AF005), which are 3C triaxial force-balance PMD SP400U3 electrochemical transducers. The 3C broadband channels (CHZ, CHN, and CHE) were oriented in the standard seismology vertical, north-south, and east-west component configurations. Broadband channels were sampled using either 250 or 500 sps, resulting in Nyquist frequencies of either 125 or 250 Hz, respectively.

6.1.2 Large N Seismic Array

A temporary seismic deployment consisting of a large number of geophones was installed for the DAG tests. This array is commonly referred to as "Large N." The Large N array includes 496 DT-SOLO 5 Hz 3C geophones. This array covers an area of approximately 2.5 km by 2 km, with a spacing of 100 m (Figure 24). Two dense lines with a spacing of 50 m are along the southwest and southeast direction. The distance from the geophones to the DAG test location ranges from approximately 200 to 2,500 m. The Large N seismic array recorded explosion data from DAG-2, DAG-3, and DAG-4. Cable-cutter data after DAG-2 and DAG-3 were also recorded.

Data recovery for the Large N seismic array is greater than 98%. The INOVA Acquisition Systems store data in a modified SEG-Y Rev. 0 format. Metadata, such as sensor locations, are all stored in the SEG-Y header. The locations are specified using UTM Zone 11 North coordinates. Channel 1 is vertical, channel 2 is east-west, and channel 3 is north-south. The microsecond part of the record time is stored in bytes 169–172. For DAG-2, 292 geophones recorded at 1,000 sps, and 199 geophones recorded at 500 sps. The origin time for the data with 1,000 sps is 18:45:56.921 and the origin time for the data with 500 sps is 18:45:57.000. For the DAG-2 cable cutters, there are 496 SEG-Y files recorded at 500 sps. For DAG-3, the data from the test and cable cutters were recorded at 500 sps in 496 SEG-Y files. Channels 1–3 are data from the test and channels 4–6 are data from the cable cutters. For DAG-4, there are 487 SEG-Y files recorded at 500 sps. Near SGZ, some channels are clipped at 2.5 Volts. The sensitivity of the sensor is 80 Volts/meter/second.

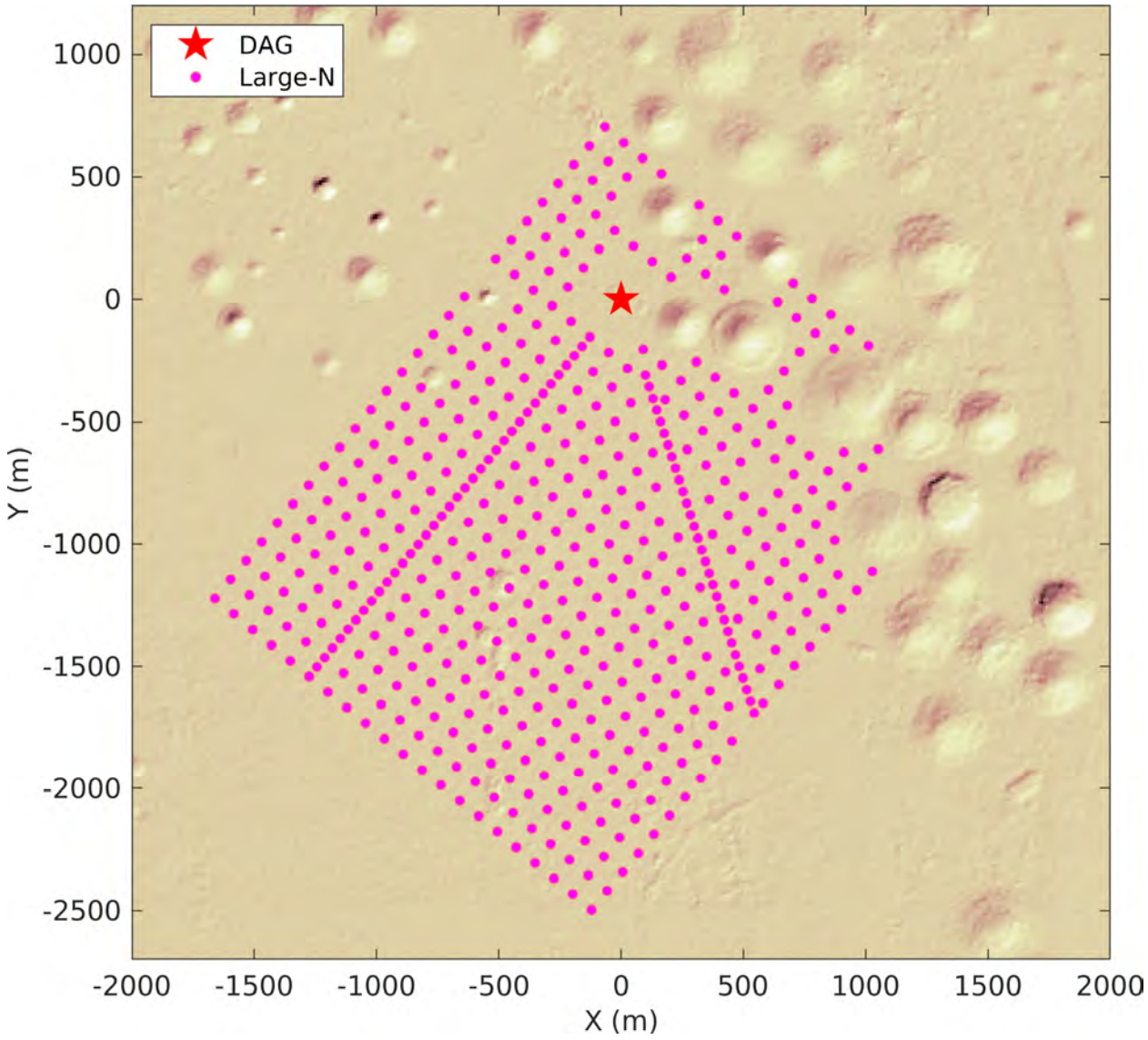

Figure 24
Layout of the Large N Seismic Array

6.2 Infrasound Instrumentation

Infrasound data were obtained by SNL for all four DAG tests using various methods as described in the following sections.

6.2.1 Primary Infrasound Array

Thirty-two Hyperion microbarometers were deployed at a range of 0.5–2 km from SGZ (Figure 25). All Hyperions located approximately 0.5 km from SGZ were the "seismically decoupled" model, which reduces the impact of spurious signals due to ground motion. Wind noise mitigation was accomplished using soaker hoses and high frequency shrouds. Hyperions at greater than 0.5 km from SGZ consisted of a mixture of seismically decoupled and non-seismically decoupled sensors. Mechanically disabled "null" Hyperion sensors were co-located at two stations within 2 km of SGZ. These sensors can be identified by channels labeled "CYF." They were disabled by removing the backing screw from the Hyperion, thereby venting the reference pressure chamber on the sensor. This made the sensor insensitive to pressure changes, meaning that all other non-pressure noise sensors (e.g., ground motion, electronic interference, etc.) are highlighted. By comparing active and null sensors at the same location, the relative contributions of non-acoustic noise sources can be assessed.

In addition to the sensors located 2 km and closer to SGZ, ten Chaparral infrasound microbarometers were deployed between 3 and 12 km from SGZ (Figure 25). Each station consisted of a single microbarometer.

The data were recorded using Ref Tek 130 digitizers sampling at 500 Hz. Data were stored locally and also telemetered to the database at UNR in near real time.

6.2.2 Downhole Microbarometer

For DAG-1 and DAG-2, these data consist of two InfraBSU microbarometers (Marcillo et al. 2012) digitized on a Reftek 130 recorder (Figures 26 and 27). One channel, DHM1 FDF, is a normally configured microbarometer (a flow filter on one port, the other port open). This prevents the unit from recording pressure signals in the infrasound or audio range frequency bands. It only records non-pressure sources. This setup can therefore distinguish between true pressure records and spurious signals from other sources such as ground motion. The other channel, DHM1 FYF, is a microbarometer with filters on both ports. There was another channel with a polarity reversed InfraBSU sensor, but it failed to record during the experiment. All sensors were installed outside of the U-2ez source hole, with aquarium tubing leading from their pressure inlets to a 2-in. diameter PVC manifold extending approximately 6.1 m (20 ft) into the source hole. The source hole was partially covered elsewhere with a mesh grate.

For DAG-3, these data consist of one InfraBSU microbarometer (Marcillo et al. 2012) digitized on a Reftek 130 recorder (Figures 26 and 27). The sensor was installed directly on the mesh grate above the source hole. It had a nominal sensitivity of 0.000046 volts per Pascal and the Ref Tek 130 had a counts-to-volts conversion of 8.61x10^-8, including the gain of 32.

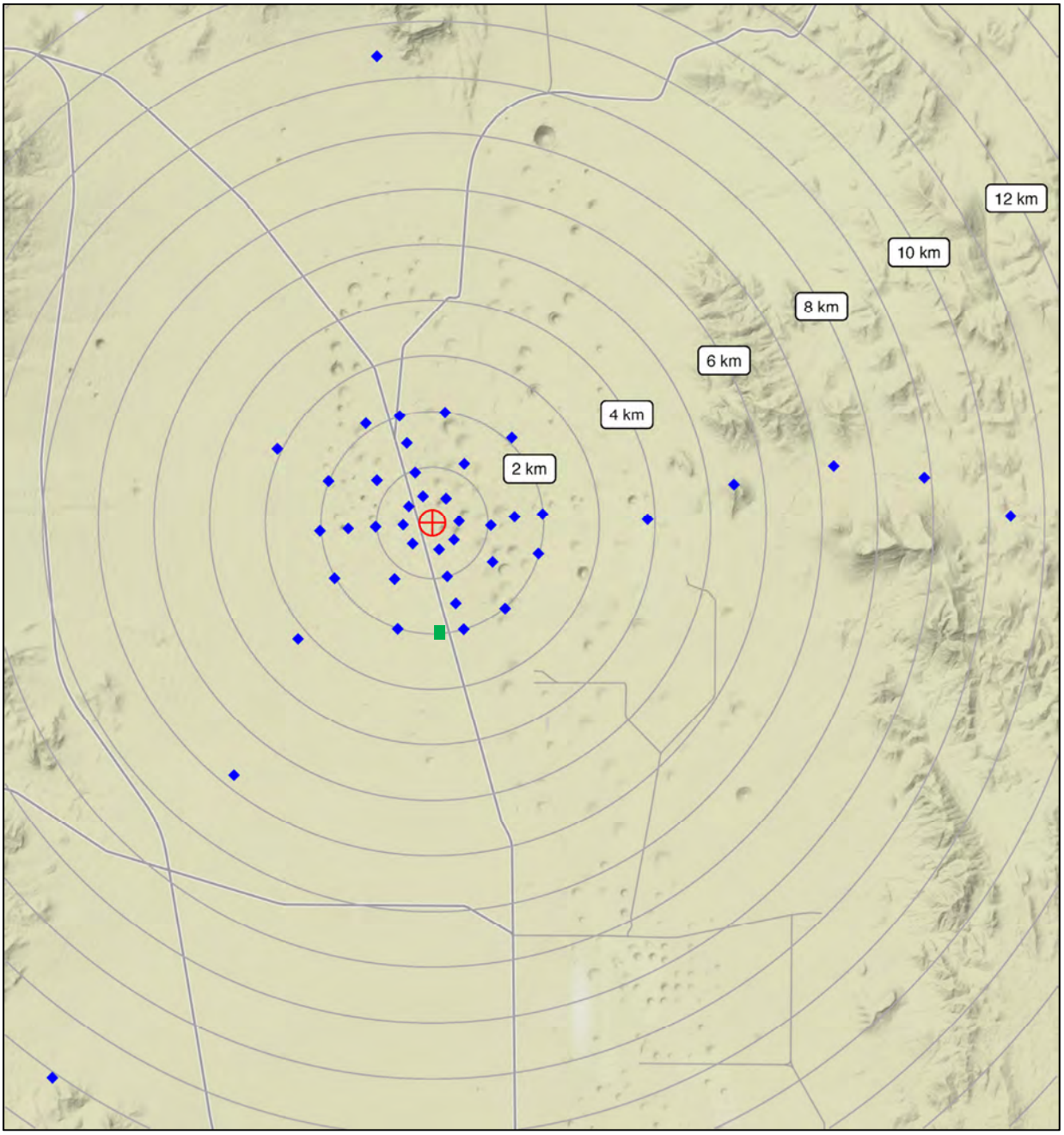

Figure 25
Map Showing Sensor Locations for the DAG Primary Infrasound Array
The horizontal distance from SGZ (red circle with cross) is labeled in kilometers. The BEEF trailer park is shown as a green rectangle.

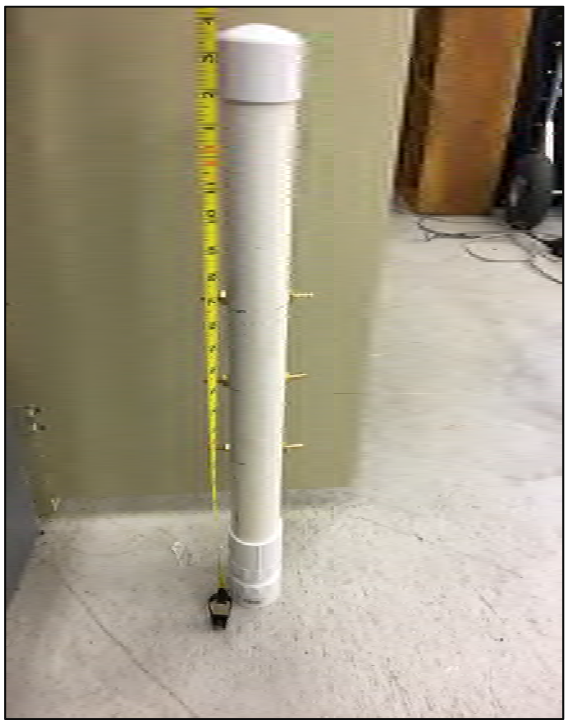

Figure 26
Microbarometer Manifold for the Downhole Pressure Recording Diagnostic
This pipe was attached to a ~10 m (33 ft) PVC pipe extending into the source hole. Aquarium tubing carried the pressure signal from the brass ports on this manifold to the microbarometers.

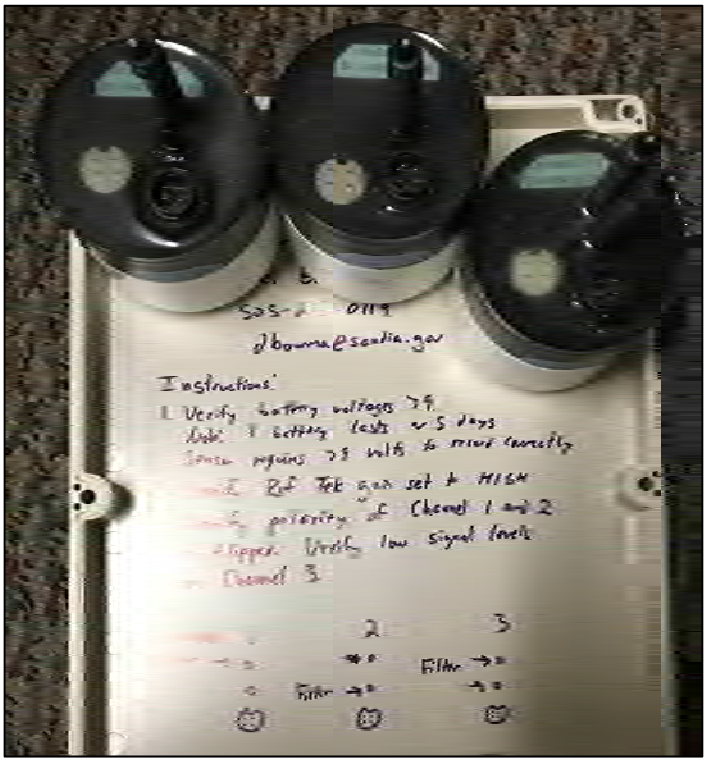

Figure 27
Configuration of the Microbarometer Recorders
Microbarometers are arranged in channel order.

6.2.3 Gem Linear Array

For DAG-1, a temporary array of Gem microbarometers (Anderson et al. 2018) was emplaced close to SGZ in an attempt to capture very faint acoustic signals that the main acoustic network may have missed. Table 2 gives the locations of the array.

Table 2
Gem Microbarometer Array Locations

Station	Latitude	Longitude	Notes
	WGS84		
GEM1	37.1147427	-116.06816	100 m from SGZ
GEM2	37.1147517	-116.06808	120 m from SGZ
GEM3	37.1147653	-116.06798	140 m from SGZ
GEM4	37.1147793	-116.06786	160 m from SGZ
GEM5	37.1147912	-116.06776	180 m from SGZ
GEM6	37.1148043	-116.06765	200 m from SGZ
GEM7	37.1148151	-116.06754	220 m from SGZ

6.2.4 Crane Microbarometer

For DAG-3, these data consist of a Gem infrasound microbarometer (Anderson et al. 2018) installed on an NNSS crane. The location of the Gem was 37.11591 north latitude, -116.07000 west longitude. The Gem was located at an elevation angle of 14.5 degrees with respect to SGZ, measured using the Theodolite app on an iPhone.

For DAG-4, these data consist of a Gem infrasound microbarometer (Anderson et al. 2018) installed on the crane. The location of the Gem was 37.11587 north latitude, -116.07 west longitude. The Gem was located 34 m (112 ft) above ground surface.

6.2.5 Balloon Microbarometer

6.2.5.1 DAG-3

For DAG-3, four infrasound microbarometer payloads were prepared for flight on heliotrope solar hot air balloons (Bowman et al. 2020). The flights were intended as “proof of concept,” since the upper air winds were expected to carry the balloons out of range of the DAG-3 infrasound signal by the time the test was executed. Thus, the data have not been exhaustively examined for potential arrivals.

Of the four payloads, Payloads 1 and 2 were brought to the launch site but were not launched. They were brought back to the nearby instrumentation trailer park (also known as “BEEF” [see location on Figure 25]) and hung from tent poles when the test was executed. The location of Payload 1 is thus marked at 37.09604 north latitude, -116.06815 west longitude. It had three channels: a normal-polarity infraBSU (channel CDF1), a reversed-polarity infraBSU (channel CDF2) and a mechanically disabled infraBSU (channel CYF). The polarity reversal is accomplished by swapping the position of the mechanical filter. The mechanically disabled channel is accomplished by removing the filters from both ports. InfraBSU microphones are described in Marcillo et al (2012).

They were digitized on a DiGOS DATA-CUBE logger. Payload 2 consisted of a Gem microbarometer and an Eagle flight computer for payload position logging. It was also located at 37.09604 north latitude, -116.06815 west longitude when DAG-3 was executed.

Payload 3 was launched on a solar hot air balloon. It had a Gem microbarometer and an Eagle flight computer for payload position logging.

Payload 4 was launched on a solar hot air balloon. It had two Gem microbarometers co-located in the same box, and an Adafruit GPS Shield for payload position logging. The GPS shield truncated all but the left two digits of the elevation reading, meaning that when the balloon reached level float, there is a +/- 1 km uncertainty in altitude.

6.2.5.2 DAG-4

For DAG-4, a total of seven infrasound microbarometer payloads were prepared for flight on heliotrope solar hot air balloons (Bowman et al. 2020). Last minute problems with the balloon trackers meant that only four were qualified for flight a day prior to the shot.

Of the seven payloads, Payload 1 and 4 were not launched. They were hung from tent poles in the BEEF trailer park when the test was executed. The location of Payload 1 is thus marked at 37.09604 north latitude, -116.06815 west longitude. It had three channels: a normal-polarity infraBSU (channel CDF1), a reversed-polarity infraBSU (channel CDF2) and a mechanically disabled infraBSU (channel CYF). The polarity reversal is accomplished by swapping the position of the mechanical filter. The mechanically disabled channel is accomplished by removing the filters from both ports. InfraBSU microphones are described in Marcillo et al. (2012). They were digitized on a DiGOS DATA-CUBE logger. Payload 4 consisted of a Gem microbarometer (Anderson et al. 2018) and an Eagle flight computer for payload position logging. It was also located at 37.09604 north latitude, -116.06815 west longitude when DAG-4 was executed. Payload 3 was not operational and was therefore not turned on.

Payload 5 was launched on a solar balloon towed aloft by a helium balloon. The solar balloon failed to deploy properly and the payload landed in the Grand Canyon prior to DAG-4. It was never recovered, as it would have required a helicopter to access the landing site.

Payload 2 was launched on a solar hot air balloon. It had a Gem microbarometer and an Eagle flight computer for payload position logging. It was located in the stratospheric shadow zone when DAG-4 was executed, and no acoustic arrivals were identified.

Payload 6 was launched on a solar hot air balloon towed aloft by a helium balloon. It had a Gem microbarometer and an Eagle flight computer for payload position logging. It was located too far to the east when DAG-4 was executed, and no acoustic arrivals were identified.

Payload 7 was launched on a solar balloon towed aloft by a helium balloon. It had a Gem microbarometer and an Eagle flight computer for payload position logging. An arrival from the DAG-4 test was identified at 21:09:27 UTC, June 22, 2019, when the balloon was at 36.68026 north latitude, -116.38151 west longitude, at an altitude of 21,867 m above mean sea level.

6.2.6 Ground Zero Microbarometer

For DAG-4, these data consist of one InfraBSU microbarometer (Marcillo et al. 2012) digitized on a Reftek 130 recorder. The sensor was installed on a post about 1 m (3 ft) tall directly over SGZ. The bitweight was 8.61x10^-8 (including the 32x gain), and the conversion for sensor volts to pascals was 0.000046.

6.3 Weather Data

Weather data were collected for the DAG tests to provide information needed for analysis of surface acoustic measurements such as infrasound. Weather data for the tests were collected from one temporary station and three permanent stations in the network of weather stations managed by the NNSS Weather Operations, Air Resources Laboratory/Special Operations and Research Division. This network is known as the SORD/NNSS Weather Mesonet, and consists of 24 stations located across the NNSS. The DAG data provided are from stations M09/A09AB, M49/A04AA, and M17/A01AB. These are 10-m (33-ft) tall towers located approximately 2.5 km northeast, 6 km south-southeast, and 2.7 km southwest, respectively, of the DAG test bed (Figure 28). Wind and other weather observations, including temperature, humidity, atmospheric pressure, and solar radiation, were taken to provide 15-minute averaged data. The temporary station, M90, was a 2-m (7-ft) tall station that recorded wind speed, wind direction, temperature, relative humidity, and atmospheric pressure every 2 seconds. This station was located approximately 2.5 km north-northwest of the DAG test bed.

In addition to the weather data collected on the 10-m (33-ft) and 2-m (7-ft) towers, SORD also collected upper air data using a radiosonde (balloon) for the DAG tests. Measurements were taken by the radiosonde every 1 second and reported every 2 seconds. Parameters recorded by the radiosonde included wind speed and direction, temperature, humidity, pressure, and location. The balloon release location was near the BEEF trailers about 2.2 km south of the DAG testbed (Figure 28).

Detailed information about the weather data collection methodology for the tests is provided in Attachment 1.

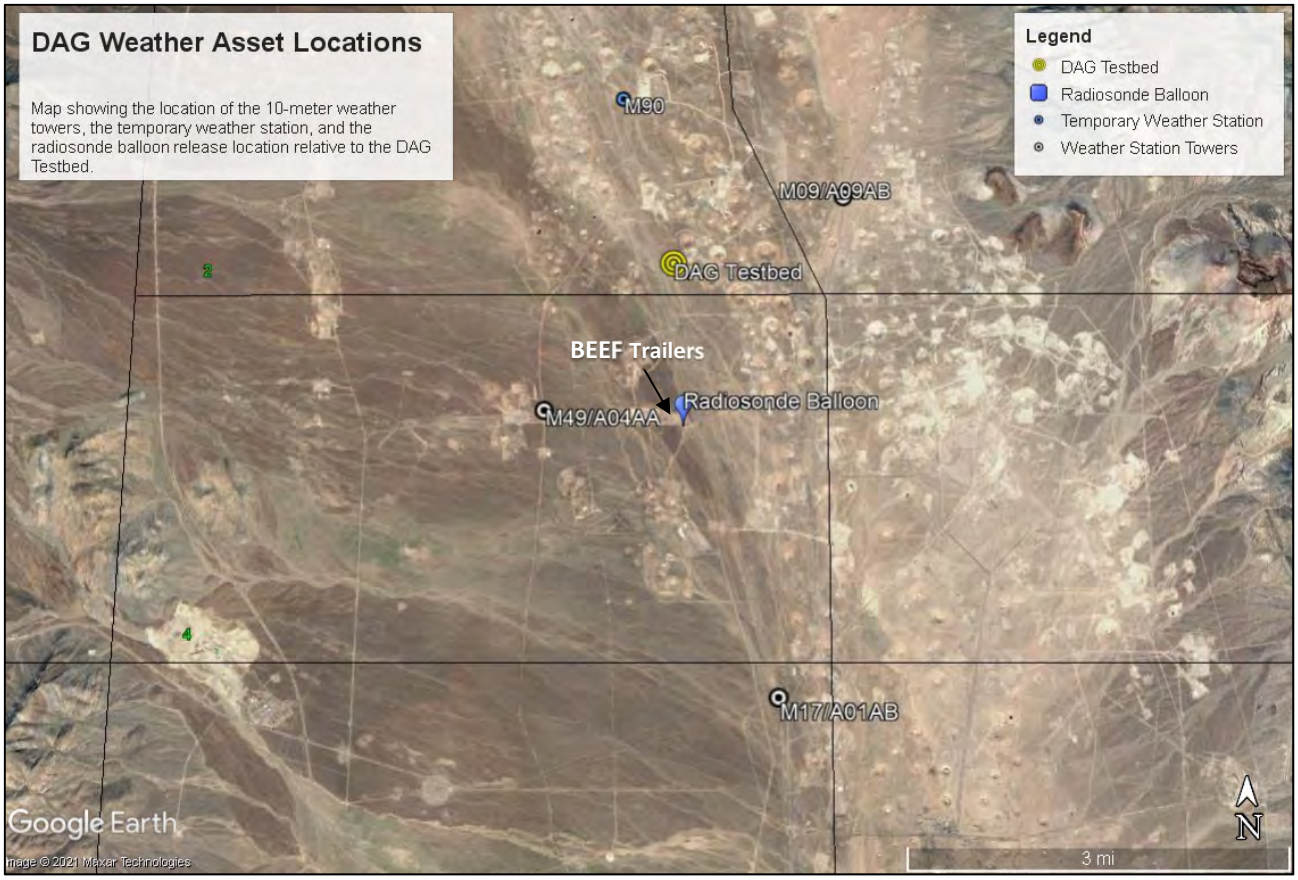

Figure 28
Google Earth Image Showing the Location of NOAA SORD Meteorological Towers and Radiosonde Balloon Release Location in Relation to the DAG Test Bed

7 Additional Diagnostics

7.1 Distributed Acoustic Sensing (DAS)

DAS technology was deployed for the DAG experiments in an effort to track continuous wavefields in addition to the few widely spaced point measurements, available from typical geophone layouts. The DAS deployed is a fiber-optic sensing system comprising an advanced optoelectronics interrogator and sensing cables. Helically-wound fiber cable (HWC) placed in two DAG boreholes in vertical seismic profiling configurations recorded up-going and down-going P and S waves. It is planned to convert the fiber strain rate to acceleration by scaling with the local apparent slowness. The technique works best in high signal-to-noise time windows where phases are well separated.

Three Silixa Carina interrogators were in place and recorded DAS data for all four DAG experiments. Interrogators 1 and 2 were attached to HWC with 30-degree pitch. Both HWC fiber runs start at a junction box located between instrumentation holes U-2ez-SW80 and E80. Interrogator 1 was run southwest from the box and inserted into borehole SW80, and interrogator 2 was run northeast from the box and inserted into borehole E80. Interrogator 3 was attached to

straight (i.e., not HWC) Silixa Constellation fiber that extended southeast from the surface junction box to the recording station over 2 km away. All surface fiber was installed in a trench up to 15 centimeters below ground surface and backfilled with native material. The downhole portions were grouted in place. Figure 29 shows a map showing the layout of the fiber optic cable lines.

The gauge length of the interrogators was 2 m (7 ft). The sample rate depended on the interrogator and the experiment, and ranged from 36 to 100 kilohertz (kHz). Full sample-rate data are not available. All data were exported by the vendor at 2,000 Hz.

Data from interrogators 1 and 2 were combined into a single SEG-Y file per experiment (file has 'HWC' in filename). Data from interrogator 3 are in a separate SEG-Y file per experiment (data have 'surface' in filename). The SEG-Y files were exported from Schlumberger Vista software and are in a Floating-Point IBM format. An effort was made to conform to SEG-Y Revision 1 standards, but some header variables may not strictly adhere. The data are in units of strain rate: nanometers/meter/second. However, due to a recording problem, the data for DAG-1 are merely proportional to strain-rate, with an unknown proportionality constant. All source and receiver locations are reported in the SEG-Y headers in UTM Zone 11 North and elevations are in WGS84 meters.

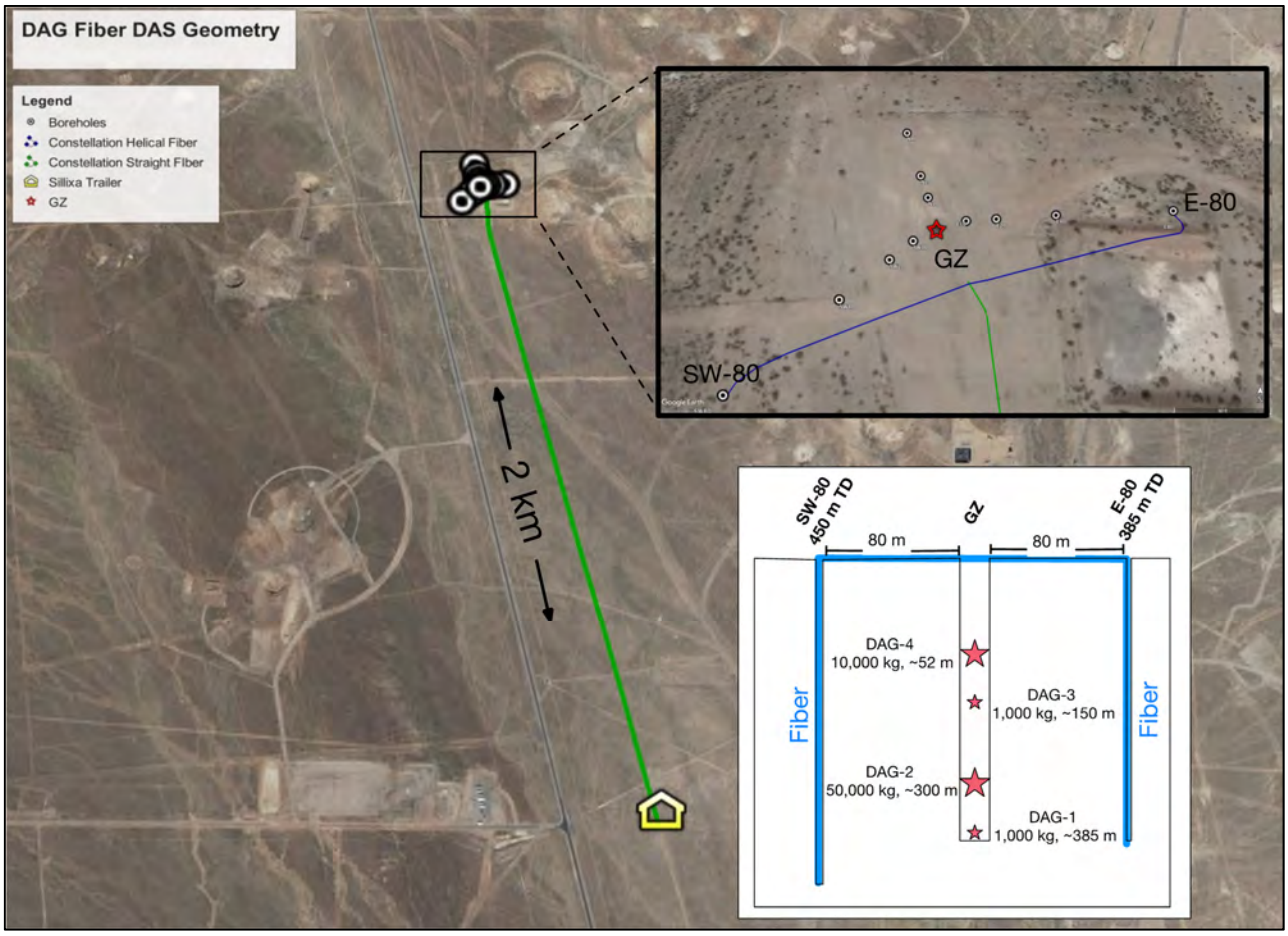

Figure 29
Map Showing the Layout of the Distributed Acoustic Sensing Fiber Optic Cable
Blue line is helically wound cable (HWC). Green line is straight Constellation fiber.

7.2 Magnetometers

7.2.1 Primary Magnetometers

Low frequency electromagnetic (EM) signals were observed from the approximately one-kiloton chemical explosion of ANFO that was part of the 1993 Non-Proliferation Experiment by Sweeney (1994). In general, chemical explosions are expected to produce low frequency EM signals (e.g. Soloviev and Sweeney 2005; Sweeney 2011). These signals are expected to attenuate rapidly, and may be observable only at close range (<1 km) from the DAG subsurface chemical explosions. The purpose of the DAG LLNL EM data collection was to observe these signals using magnetometers deployed at close range (<100 m).

These observations are complicated by several factors: 1) movement of the sensors in the Earth's ambient field will create signals; 2) timing and firing circuits may produce signals; and 3) high background noise due to power lines and other sources of EM energy. These difficulties may be mitigated by co-locating the magnetometer with a seismic sensor and by the collection of background data prior to the test and during the dry runs, when much, but not all, of the timing and firing circuitry is tested.

The observations were made by deploying magnetometers (B field) sensors near SGZ. Two setups, at distances of 30 and 60 m (horizontal distance from SGZ), were installed for each test (Figure 30 and Table 3). Each setup consisted of three orthogonal B field sensors (EMI BF-5/6 magnetometers) with coil windings and a nominal response of 1–100 kHz (Figure 31). A seismic sensor, typically a KMI EpiSensor, was installed at each location as well, to measure ground motion, because the arrival of the seismic wave will produce signals due to the motion of the sensor within the Earth's magnetic field. A seismic sensor is essential for proper interpretation of the data (e.g., Sweeney 2011) and to ensure that that signal associated with later-arriving ground motion can be distinguished from the actual source EM signal, which arrives earlier due to higher propagation speed of the EM signals (~3e10 m/s) as opposed to the seismic signals (~3e4 m/s).

Data were recorded on a six channel Reftek at 500 or 1000 sps. The Reftek uses a non-causal finite impulse response (FIR) anti-alias filter, which may produce acausal transients for high-frequency signals near the Nyquist frequency. The exact response of the FIR differs with the firmware version. Timing is based on a crystal oscillator with periodic locks to an external GPS signal.

Table 3
Positions of Primary DAG Magnetometer Sensors

Reftek	Latitude (DMS)	Longitude (DMS)	Elevation
B258	37 13 14.69	116 03 40.29	1,520 m (4,987 ft)
B259	37 13 13.72	116 03 40.80	1,523 m (4,997 ft)

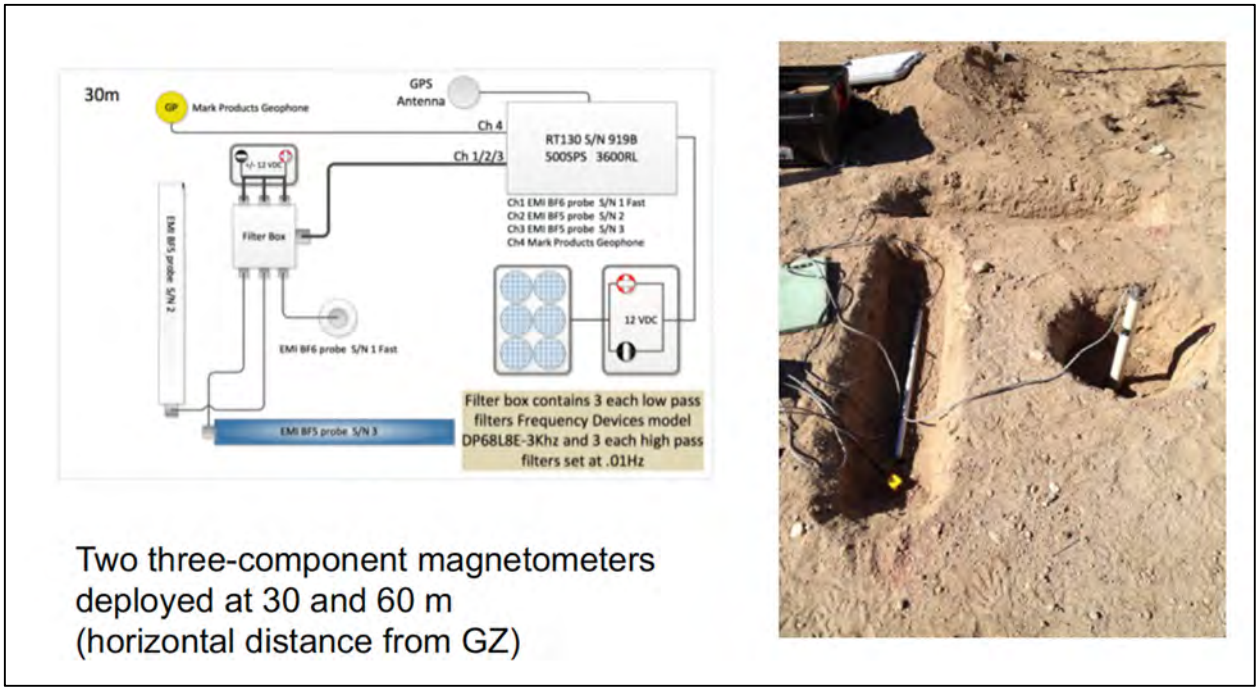

Figure 30
Primary Magnetometer Set-up at Each Point
Magnetometer schematic shown in left image. Right image shows co-located magnetometer and EpiSensor seismic sensor.

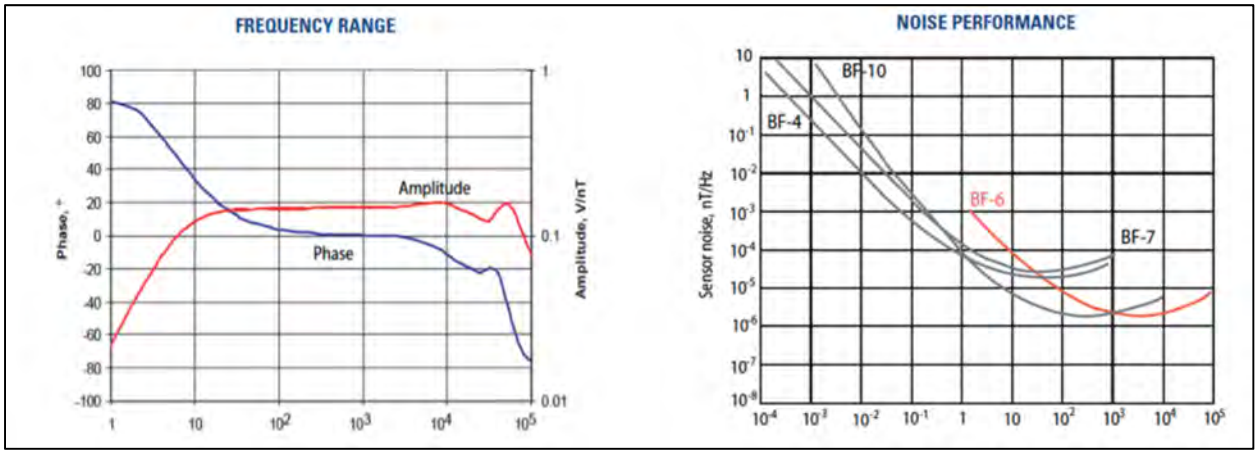

Figure 31
Nominal Frequency and Amplitude Response for the Primary DAG Magnetometers

7.2.2 Atomic Magnetometers

Two QTFM QuSpin scalar magnetic field sensors were deployed for DAG-4. The sensors recorded the total magnetic field and their GPS time and position. See Table 4 for sensor locations. These can also be recovered from the QTFM files and from the code in p01_ReadPlotDag4Data.py. The sensors were about one meter closer to SGZ than listed because the GPS antenna was not on the magnetometer.

There are no known issues with the data. Python 3 code is included with the data to show how it was processed. The raw data recorded directly from the sensors are in ./rawData. It is plain text. The Python code p00_cleanTheRawData.py removes null bytes from the raw files and dumps that data into ./cleanData. The Python code p01_ReadPlotDag4Data parses the clean data into two sets of data: magnetometer and GPS. The GPS data are used to align the clock in the magnetometer data to the GPS PPS (pulse per second). This means timing is probably no more accurate than the sampling frequency of the sensors, which is ~1/204 Hz ~= 4 milliseconds.

Table 4
Atomic Magnetometer Locations for DAG-4

Sensor	Latitude	Longitude
	WGS84	
Northeast	37.115020	-116.069024
Southeast	37.114394	-116.068796

7.3 Unmanned Aerial System (UAS) Photogrammetry

The low-altitude aerial photogrammetry diagnostic was designed to capture high-resolution overhead imagery with surface ground control in order to develop detailed topographic models before and after select experiments in the DAG series. This diagnostic facilitated the identification, quantification, and analyses of any surface changes generated as a result of the underground conventional high-explosive experiments. This diagnostic involved the deployment of a commercial-off-the-shelf digital single-lens reflex (DSLR) camera, fixed to a small unmanned aerial vehicle and deployed at low altitude (<40 m above ground level). The vehicle plus the sensor is referred to as an unmanned aerial system (UAS). Imagery was collected in a pre-defined boustrophedonic pattern over a region of 820 m by 720 m (~3,160 m^2). The centroid location of the diagnostic collection area is off-centered with respect to SGZ in order to explore any surface changes distal to SGZ that may be associated with nearby topographic relief (e.g., legacy underground nuclear explosion collapse craters adjacent to the DAG site) and buried faults. To obtain the highest possible resolution elevation data, imagery was collected with significant overlap (>80% frontal overlap and >65% side overlap) and in conjunction with a dense network of geodetically-surveyed ground control points. The pre-experiment data were collected over a three- to five-day period preceding the experiments, and post-experiment data were collected as soon as site conditions were deemed safe and accessibility was granted following the experiment execution (typically within 1-2 days). Image data were photogrammetrically processed using Agisoft Photoscan (now Agisoft Metashape), orthorectified, and rendered into digital elevation models in conjunction with the surveyed ground control points in order to develop orthorectified composite orthoimages and topographic data products that could be compared against each other to determine and assess surface changes.

Further details on the diagnostic deployment (including aircraft and camera sensor specifications) and data analysis methods can be found in Crawford et al. (2021), https://www.mdpi.com/2504-446X/5/2/25/htm. Example maps, deployment methodological discussions, data processing

methodological information, data quality thresholds, and details on image quality can also be found in Crawford et al. (2021). Interested parties are referred first to this open-access peer-reviewed manuscript as a resource, and encouraged to contact the authors of that paper for further details on the current state of these data and related ongoing research, and with any questions.

Raw image data are available for the DAG-2 and DAG-4 experiments, and can be obtained on request to specific staff (listed below) in the Los Alamos National Laboratory's Earth Systems Observations Group. Approximately 32,000 individual image files exist in total, for an aggregate total data volume of 1.2 terabytes. The DAG-2 photogrammetric campaign collected approximately 11,000 total pre-experiment and post-experiment photos, while the DAG-4 photogrammetric campaign collected about 18,500 pre-experiment and approximately 19,500 post-experiment photos. Photogrammetric analyses for DAG-4 additionally included a much later-time post-experiment data collection, which took place approximately six weeks after the experiment, and that dataset consists of approximately 8,500 photos. For both the DAG-2 and DAG-4 campaigns, the imagery link to absolute spatial change via a network of at least 220 surveyed ground control points. These fiducials were installed and surveyed before the pre-experiment photogrammetric data collection, and surveyed again following the post-experiment photogrammetric collections.

Raw image files, processed pre- and post-experiment ortho-imagery, pre- and post-experiment digital elevation models, and ground control point survey information can be obtained by contacting the following:

- Brandon Crawford (bcrawford@lanl.gov)
- Anita Lavadie-Bulnes (lavabul@lanl.gov)
- Emily Schultz-Fellenz (eschultz@lanl.gov)
- Erika Swanson (emswanson@lanl.gov)

7.4 Fully Polarimetric Synthetic Aperture Radar Imagery (PolSAR)

PolSAR data were collected for DAG-2 on December 19, 2018 by airplane with the SNL Facility for Advanced RF and Algorithm Development (FARAD) X-band (9.6 gigahertz center frequency) SAR system in circular trajectory videoSAR mode. The airplane flew two circles before DAG-2, one circle during DAG-2, and two circles after DAG-2. The data sets used were the first circle flown before DAG-2 (denoted as C_{-2}), the circle flown during DAG-2 (denoted as C_0), and the second circle flown after DAG-2 (denoted as C_{+2}). The data set contains calibrated fully-polarimetric images with the linear polarization channels:

- vertical receive, vertical transmit (VV)
- horizontal receive, vertical transmit (HV)
- vertical receive, horizontal transmit (VH)
- horizontal receive, horizontal transmit (HH)

A short list of the nominal collection and imaging parameters are as follows:

- Desired grazing = 38.0 degrees
- Desired standoff range = 3,470 m
- Image resolution = 0.1016 m in slant-range and cross-range resolution after a -35 dB Taylor weighting
- Pixel spacing = 0.07816 m
- Desired scene size dimensions = 200 m in slant-range and cross-range

MATLAB code will be supplied to read the imagery format.

Included files:

- Formed complex-valued images for apertures used. Data are real and imaginary reflective values, not amplitude and phase. The images from C_{-2} and C_{+2} are co-registered to the images from C_0.
- Coherence between apertures from C_{-2} and C_0, and C_0 and C_{+2}.
- H/A/α polarimetric decomposition for apertures in the same circles given above. The decomposition is described in Yocky et al. (2019).

Initial exploitation and results from the data set are captured in West et al. (2021). A sample data set consisting of approximately 700 megabytes will be posted to IRIS. The total data set is approximately 46 gigabytes. The data have been approved as unclassified unlimited release (UUR) by SNLs review and approval process. The entire data set will be hosted at SNL. For SNL images, the copyright statement is: © 2021 National Technology & Engineering Solutions of Sandia, LLC, and should be used in any publication.

7.5 Video

Several types of videos were obtained during the DAG tests by LANL and MSTS, as described in the following sections.

7.5.1 U-2ez Site Camera and GoPro Cameras

Two types of videos, test detonation and cable-cutter, were obtained by LANL for the DAG tests using LANL's U-2ez site camera and GoPro cameras. Video footage was collected during each experiment to observe the event and to record the degree to which the cables suspending the explosives canisters in the U-2ez source hole were disrupted by the detonation. Attachment 2 provides a complete descriptive document, which is summarized in this section, containing photos and a list of videos and camera settings.

Each experiment canister was suspended from a pair of wire cables in the source hole. As described in Section 4, the hole was stemmed with gravel, sand, and grout above each canister prior to detonation. Because of this, the cables showed minimal motion during the events. The canister for DAG-4 was installed near the top of the source hole and the hole was stemmed to ground level, so cables were not present for DAG-4. Cable-cutter videos were collected during ancillary explosive operations that followed DAG-1, DAG-2, and DAG-3. Each operation utilized small shaped charges with Composition C-4 to cut the cables just above the top of stemming for the three experiments.

More motion of the cables was observed during the cable-cutter operations than during the tests due to the release of tension that was applied during installation of the experiment canisters.

Thirteen videos were collected by LANL. They are available upon request from Juan-Antonio Vigil (jvigil47@lanl.gov).

7.5.2 High-Speed Video Cameras and Handy-Cams

MSTS fielded two high-speed Phantom V711 cameras (S/N: 11894 and S/N: 13546) and four handy-cams (HC-01, HC-02, HC-03, and HC-04) for each of the DAG tests and also the cable cutter events. The goal of fielding both high-speed and low-speed video was to capture any ground motion, determine estimates of shock propagation, determine symmetry of shock propagation, and also record any late-time events that may have occurred at the U-2ez test bed and the surrounding area from different vantage points. Attachment 3 provides the complete descriptive document, which is summarized in this section, containing findings, photos, and lists of videos, camera settings, and camera locations.

Both high-speed video cameras were located west of U-2ez in a large enclosure (known as the "Ice Box"), which was temperature controlled and had a viewport on the side covered by plexiglass so no wind or debris would interrupt the view of the cameras. It also housed all of the equipment necessary to communicate with the systems remotely from the BEEF trailer park (located about 2.2 km south of U-2ez). In order to mitigate any sort of ground vibration coming from the equipment so it would not affect the seismic recording equipment around U-2ez, all of the equipment in the Ice Box trailer were running either off of a RUPS unit or dedicated battery supplies for the high-speed cameras. The handy-cams were positioned roughly north, east, and west, and at U-2ez at varying distances depending upon the event itself.

A total of 36 videos were collected by MSTS. They are available upon request from Rand Kelly (kellyrp@nv.doe.gov).

8 Post-Experiment Procedures

Post-experiment aggregation, merging, archiving, and distribution of data from DAG-1 through DAG-4 were conducted at UNR by the technical members of the NSL. The process employed the Antelope Real Time and data processing software system from Boulder Real Time Technologies (Boulder, Colorado); the data processing suite from the Program for Array Seismic Studies of the Continental Lithosphere (PASSCAL); the CSS 3.0 database format; and Ubuntu-Linux-based servers at NSL data centers.

9 Summary

This report coincides with the official release of near- and far-field seismic, acoustic, and diagnostic data for DAG-1, DAG-2, DAG-3, and DAG-4. The report includes a description of the experiment, the types of data and instruments, and post-experiment data processing. This data release includes separate sets of these data, including the raw data as well as the data reflecting the application of the corrections.

10 Acknowledgements

DAG would not have been possible without the support of many people from several organizations. The authors wish to express their gratitude to the U.S. Department of Energy, National Nuclear Security Administration, Defense Nuclear Nonproliferation Research and Development and the DAG working group, a multi-institutional and interdisciplinary group of scientists and engineers. Deepest appreciation is given to Robert White and Kale McLin (MSTS) for their tireless work on the seismic array, and to the NSL at UNR for their support of the seismic network and for data aggregation.

This work was done by MSTS under Contract No. DE-NA0003624.

11 References

Anderson, J. F., J. B. Johnson, D. C. Bowman, and T. J. Ronan, 2018. "The Gem Infrasound Logger and Custom-Built Instrumentation." *Seismological Research Letters*. Vol. 89, No. 1, pp. 153–164**,** https://doi.org/10.1785/0220170067.

Bechtel Nevada, 2006. *A Hydrostratigraphic Model and Alternatives for the Groundwater Flow and Contaminant Transport Model of Corrective Action Unit 97: Yucca Flat–Climax Mine, Lincoln and Nye Counties, Nevada*. DOE/NV/11718--1119. Las Vegas, NV.

Bowman, D.C., 2019. "Yield and Emplacement Depth Effects on Acoustic Signals from Buried Explosions in Hard Rock." *Bulletin of the Seismological Society of America*. Vol. 109, No. 3, pp. 944–958, https://doi.org/10.1785/0120180285.

Bowman, D. C., P. E. Norman, M. T. Pauken, S. A. Albert, D. Dexheimer, X. Yang, S. Krishnamoorthy, A. Komjathy, and J. A. Cutts, 2020. "Multihour Stratospheric Flights with the Heliotrope Solar Hot-Air Balloon." *Journal of Atmospheric and Oceanic Technology*. Vol. 37, No. 6, pp. 1051–1066, https://doi.org/10.1175/JTECH-D-19-0175.1.

Blom, P., A. Iezzi, and G. Euler, 2020. "Seismoacoustic analysis of underground explosions using the Rayleigh integral." *Geophysical Journal International.* Vol. 223, No. 2, pp. 1,069–1,085, https://doi.org/10.1093/gji/ggaa363.

Chen, T., C. M. Snelson, and R. Mellors, 2020. "Velocity Structure at the Source Physics Experiment Phase I Site Obtained with the Large-N Array Data." *Seismological Research Letters*. Vol. 91, No. 1, pp. 304–309, https://doi.org/10.1785/0220190104.

Cole, J. C. and P. H. Cashman, 1999. *Structural Relationships of Pre-Tertiary Rocks, Nevada Test Site Region, Southern Nevada*. U.S. Geological Survey Professional Paper 1607.

Cronkite-Ratcliff, C., G. A. Phelps, and A. Boucher, 2012. *A Multiple-Point Geostatistical Method for Characterizing Uncertainty of Subsurface Alluvial Units and its Effect on Flow and Transport*. U.S. Geological Survey Open-File Report 2012–1065.

Crawford, B., E. Swanson, E. Schultz-Fellenz, A. Collins, J. Dann, E. Lathrop, and D. Milazzo, 2021. "A New Method for High Resolution Surface Change Detection: Data Collection and Validation of Measurements from UAS at the Nevada National Security Site, Nevada, USA." *Drones*. Vol. 5, No. 2, 20 pages, https://doi.org/10.3390/drones5020025.

Ford, S. R. and O. Y. Vorobiev, 2020. “Characterization of Spall in Hard Rock from Observations and Simulations of the Source Physics Experiment Phase I.” *Bulletin of the Seismological Society of America.* Vol. 110, No. 2, pp. 596–612, https://doi.org/10.1785/0120190214.

Ford, S. R. and W. R. Walter, 2021. “Source Separation and Medium Change of Contained Chemical Explosions from Coda Wave Interferometry.” *The Seismic Record.* Vol. 1, No. 1, pp. 3–10, https://doi.org/10.1785/0320210002.

Ford, S., and W. R. Walter, 2013. “An Explosion Model Comparison with Insights from the Source Physics Experiments.” *Bulletin of the Seismological Society of America*. Vol. 103, No. 5, pp. 2937–2945, https://doi.org/10.1785/0120130035.

Howard, N. W., 1980. *U2eq: Preliminary Site Characteristics Summary*. Lawrence Livermore National Laboratory Report DM 80-41.

Huckins-Gang, H. and S. Drellack, 2016. *Drilling, Completion, and Geology of Argon holes U-2ez-Ar-1 and U-2ez-Ar-2*. National Security Technologies, LLC unpublished report. Las Vegas, NV.

Huckins-Gang, H. and K. Wagner, 2017. *Geomorphic Surfaces and Associated Soils at the Source Physics Experiment Phase II Dry Alluvium Geology (DAG) Site: A Preliminary Investigation*. National Security Technologies, LLC unpublished report. Las Vegas, NV.

Ichinose, G. A., S. R. Ford, K. A. Kroll, D. A. Dodge, M. L. Pyle, A. Pitarka, and W. R. Walter, 2021. “Preliminary Analysis of Source Physics Experiment Explosion-Triggered Microseismicity using the Back-Projection Method.” *Journal of Geophysical Research*: *Solid Earth*. Vol. 126, No. 5, https://doi.org/10.1029/2020JB021312.

Marcillo, O., J. B. Johnson, and D. Hart, 2012. “Implementation, Characterization, and Evaluation of an Inexpensive Low-Power Low-Noise Infrasound Sensor Based on a Micromachined Differential Pressure Transducer and a Mechanical Filter.” *Journal of Atmospheric and Oceanic Technology*. Vol. 29, No. 9, pp. 1275–1284, https://doi.org/10.1175/JTECH-D-11-00101.1.

Marvin, R. F., H. H. Mehnert, and C. W. Naeser, 1989. “U.S. Geological Survey Radiometric Ages – Compilation ‘C’, Part Three – California and Nevada.” *Isochron/West*, No. 52, pp. 3–11.

Mission Support and Test Services, LLC, 2019. *Data Release Report for Source Physics Experiments 5 and 6 (SPE-5 and SPE-6), Nevada National Security Site*. DOE/NV/03624--0524. Las Vegas, NV.

MSTS, Mission Support and Test Services, LLC

National Security Technologies, LLC, 2014. *Data Release Report for Source Physics Experiment 1 (SPE-1), Nevada National Security Site*. DOE/NV/25946--2018. Las Vegas, NV.

National Security Technologies, LLC, 2017. *Data Release Report for Source Physics Experiment 4Prime (SPE-4Prime), Nevada National Security Site*. DOE/NV/25946--3266, Rev. 1. Las Vegas, NV.

NSTec, see National Security Technologies, LLC.

Pasyanos, M. E., and K. Kim, 2019. “Seismoacoustic Analysis of Chemical Explosions at the Nevada National Security Site.” *Journal of Geophysical Research: Solid Earth*. Vol. 124, No. 1, pp. 908–924, https://doi.org/10.1029/2018JB016705.

Phelps, G. A., A. Boucher, and K. J. Halford, 2011. *A Refined Characterization of the Alluvial Geology of Yucca Flat and its Effect on Bulk Hydraulic Conductivity*. U.S. Geological Survey Open-File Report 2010–1307.

Pitarka, A. and R. Mellors, 2021. "Using Dense Array Waveform Correlations to Build a Velocity Model with Stochastic Variability." *Bulletin of the Seismological Society of America*. Vol. 111, No. 4, pp. 2021–2041, https://doi.org/10.1785/0120200206.

Poppeliers, C., L. B. Wheeler, and L. Preston, 2020. "The Effects of Atmospheric Models on the Estimation of Infrasonic Source Functions at the Source Physics Experiment." *Bulletin of the Seismological Society of America.* Vol. 110, No. 3, pp. 998–1010, https://doi.org/10.1785/0120190241.

Preston, L., C. Poppeliers, and D. J. Schodt, 2020. "Seismic Characterization of the Nevada National Security Site Using Joint Body Wave, Surface Wave, and Gravity Inversion." *Bulletin of the Seismological Society of America*. Vol. 110, No. 1, pp. 110–126, https://doi.org/10.1785/0120190151.

Pyle, M. L., and W. R. Walter, 2019. "Investigating the Effectiveness of P/S Amplitude Ratios for Local Distance Event Discrimination." *Bulletin of the Seismological Society of America*. Vol. 109, No. 3, pp. 1071–1081, https://doi.org/10.1785/0120180256.

Sawyer, D. A., J. J. Fleck, M. A. Lanphere, R. G. Warren, and D. E. Broxton, 1994. "Episodic Caldera Volcanism in the Miocene Southwest Nevada Volcanic Field: Revised Stratigraphic Caldera Framework, 40Ar/39Ar Geochronology, and Implications for Magmatism and Extension." *Geological Society of America Bulletin*. Vol. 67, No. 10, pp. 1304–1318.

Scalise, M., A. Pitarka, J. N. Louie, and K. D. Smith, 2021. "Effect of Random 3D Correlated Velocity Perturbations on Numerical Modeling of Ground Motion from the Source Physics Experiment." *Bulletin of the Seismological Society of America*. Vol. 111, No. 1, pp. 139–156, https://doi.org/10.1785/0120200160.

Schultz-Fellenz, E., E. M. Swanson, A. J. Sussman, R. T. Coppersmith, R. E. Kelley, E. D. Miller, B. M. Crawford, A. F. Lavadie-Bulnes, J. R. Cooley, S. R. Vigil, M. J. Townsend, and J. M. Larotonda, 2020. "High resolution surface topographic change analyses to characterize a series of underground explosions." *Remote Sensing of Environment*. Vol. 246, No. 1, 23 pages, https://doi.org/10.1016/j.rse.2020.111871.

Slate, J. L., M. E. Berry, P. D. Rowley, C. J. Fridrich, K. S. Morgan, J. B. Workman, O. D. Young, G. L. Dixon, V. S. Williams, E. H. McKee, D. A. Ponce, T. G. Hildenbrand, WC Swadley, S. C. Lundstrom, E. B. Ekren, R. G. Warren, J. C. Cole, R. J. Fleck, M. A. Lanphere, D. A. Sawyer, S. A. Minor, D. J. Grunwald, R. J. Laczniak, C. M. Menges, J. C. Yount, and A. S. Jayko, 1999. *Digital Geologic Map of the Nevada Test Site and Vicinity, Nye, Lincoln, and Clark Counties, Nevada and Inyo County, California*. U.S. Geological Survey Open-File Report 99-554-A, scale 1:120,000.

Snelson, C. M., V. D. Chipman, R. L. White, R. F. Emmitt, M. J. Townsend, D. L. Barker, and P. Lee, 2012. "An Overview of the Source Physics Experiment at the Nevada National Security Site." In: *Proceedings of the 2012 Monitoring Research Review: Ground-Based Nuclear Explosion Monitoring Technologies, Volume I*. Albuquerque, NM.

Snelson, C. M., R. Mellors, H. J. Patton, A. J. Sussman, M. J. Townsend, and W. R. Walter, 2013. "Source Physics Experiments to Validate a New Paradigm for Nuclear Test Monitoring." *Eos, Transactions, American Geophysical Union*. Vol. 94, No. 27, pp. 237–239.

Snelson, C. M., C. R. Bradley, W. R. Walter, T. Antoun, R. Abbott, K. Jones, V. Chipman, and L. Montoya, 2019. *The Source Physics Experiment (SPE) Science Plan*, Version 2.4c, 23 pages, Lawrence Livermore National Laboratory Technical Report LLNL-TR-654513.

Soloviev, S. P. and J. J. Sweeney, 2005. “Generation of electric and magnetic field during detonation of high explosive charges in boreholes.” *Journal of Geophysical Research*. Vol. 110, No. B1, https://doi.org/10.1029/2004JB003223.

Swanson, E., J. Wilson, S. Broome, and A. Sussman, 2020. “The Complicated Link between Material Properties and Microfracture Density for an Underground Explosion in Granite.” *Journal of Geophysical Research: Solid Earth*. Vol. 125, No. 11, https://doi.org/10.1029/2020JB019894.

Sweeney, J. J., 1994. “Low-Frequency Electromagnetic Measurements at the NPE and Hunter’s Trophy: A Comparison.” In: *Proceedings of the Symposium on the Non-Proliferation Experiment*, April 19-21, 1994, Rockville, MD, U.S. Department of Energy document CONF-9404100, pp. 8-21–8-33.

Sweeney, J. J., 2011. *Low Frequency Electromagnetic Pulse and Explosions*. Lawrence Livermore National Laboratory Technical Report LLNL-TR-471856.

Sweetkind, D. S. and R. M. Drake II, 2007. *Geologic Characterization of Young Alluvial Basin-fill Deposits from Drill-hole Data in Yucca Flat, Nye County, Nevada*. U.S. Geological Survey Scientific Investigations Report 2007–5062.

U.S. Department of Energy, National Nuclear Security Administration Nevada Field Office, 2015. *United States Nuclear Tests, July 1945 through September 1992*. DOE/NV--209, Revision 16. Las Vegas, NV.

Vorobiev, O. Y. and M. B. Rubin, 2021a. “Modeling the dynamic response of rock masses with multiple compliant fluid saturated joint sets − Part: II Continuum modeling.” *International Journal of Impact Engineering*. Vol. 150, 14 pages, https://doi.org/10.1016/j.ijimpeng.2020.103746.

Vorobiev, O. Y. and M. B. Rubin, 2021b. “Modeling the dynamic response of rock masses with multiple compliant fluid saturated joint sets – Part I: Mesoscale simulations.” *International Journal of Impact Engineering*. Vol. 151, 15 pages, https://doi.org/10.1016/j.ijimpeng.2020.103747.

Wagner, K., H. Huckins-Gang, L. Prothro, 2017. *Drilling of the Dry Alluvium Geology (DAG) Instrument Boreholes at U-2ez in Yucca Flat, Nevada National Security Site, Nye County, Nevada*. National Security Technologies, LLC unpublished report. Las Vegas, NV.

Wagoner, J. L. and H. L. McKague, 1985. “Variation of Physical Properties of Alluvium in an Arid Basin.” *Sedimentary Geology*. Vol. 47, pp. 53–68.

West, R. D., R. E. Abbott, and D. A. Yocky, 2021. “Comparison of Surface Phenomena Created by Underground Chemical Explosions in Dry Alluvium and Granite Geology from Fully-Polarimetric VideoSAR Data.” *IEEE Journal of Selected Topics in Applied Earth Observations and Remote Sensing*. Vol. 14, pp. 6165–6178, https://doi.org/10.1109/jstars.2021.3087909.

Yocky, D. A., R. D. West, R. M. Riley, and T. M. Calloway, 2019. "Monitoring Surface Phenomena Created by an Underground Chemical Explosion Using Fully Polarimetric VideoSAR.” *IEEE Transactions on Geoscience and Remote Sensing*. Vol. 57, No. 5, pp. 2481–2493, https://doi.org/10.1109/TGRS.2018.2873979.

Yocky, D. A., R. D. West, and R. E. Abbott, 2021. “Comparison of PolSAR Surface Measurements from Underground Chemical Explosions to Recorded and Predicted Surface Ground Motion.” *IEEE Journal of Selected Topics in Applied Earth Observations and Remote Sensing*. Vol. 14, pp. 165–174, https://doi.org/10.1109/JSTARS.2020.3031684.

Appendix 1

Construction Data for Boreholes Drilled at the U-2ez Site

Appendix 1
Construction Data for Boreholes Drilled at the U-2ez Site

Hole Name	Spud Date	Completion Date	Accelerometer Install Date	Stem Date	Azimuth from Source Hole (degrees)	Distance from Source Hole (ft)	Conductor Hole		Conductor Casing		Borehole		SPC (NAD27/NGVD29)			Notes
							Diameter (in.)	Depth (ft)	Diameter (in.)	Depth (ft)	Diameter (in.)	Depth (ft)	Northing (sft)	Easting (sft)	TOC Elev (sft)	
U-2ez	8-Nov-1983	20-Nov-1983	na	na	na	na	98	118	98	117	96	1300	861,270.23	674,440.22	4,216.52	NNSS Survey 12/12/16
U-2ez N10	2-May-2017	3-May-2017	14-Feb-2018	14-Mar-2018	342	32.73	18	81	13.375	83.05	10.625	1322.84	861,301.33	674,430.02	4,216.00	NNSS Survey 10/4/18
U-2ez N20	30-Mar-2018	3-Apr-2017	28-Feb-2018	14-Mar-2018	342	65.53	18	87	13.375	83.75	10.625	1334.16	861,332.72	674,420.48	4,215.86	NNSS Survey 10/4/18
U-2ez N40	3-Apr-2017	6-Apr-2017	6-Mar-2018	2-May-2018	342	131.04	18	85	13.375	82.90	10.625	1330.00	861,395.10	674,400.48	4,216.03	NNSS Survey 10/4/18
U-2ez N80	7-Apr-2017	11-Apr-2017	26-Mar-2018	2-May-2018	342	262.22	18	85	13.375	80.97	10.625	1336.51	861,520.08	674,360.64	4,219.67	NNSS Survey 10/4/18
U-2ez E10	24-Apr-2017	27-Apr-2017	22-Feb-2018	14-Mar-2018	85	32.84	18	87	13.375	82.80	10.625	1332.24	861,273.28	674,472.92	4,215.74	NNSS Survey 10/4/18
U-2ez E20	28-Mar-2017	29-Mar-2017	22-Feb-2018	14-Mar-2018	85	65.91	18	87	13.375	83.50	10.625	1330.18	861,275.78	674,505.89	4,215.82	NNSS Survey 10/4/18
U-2ez E40	17-Apr-2017	19-Apr-2017	7-Mar-2018	2-May-2018	85	131.40	18	83.5	13.375	81.00	10.625	1330.00	861,281.28	674,571.15	4,215.14	NNSS Survey 10/4/18
U-2ez E80	19-Apr-2017	24-Apr-2017	9-Apr-2018	2-May-2018	85	262.53	18	85	13.375	80.71	10.625	1330.28	861,292.09	674,701.84	4,214.83	NNSS Survey 10/4/18
U-2ez SW10	27-Apr-2017	1-May-2017	26-Feb-2018	14-Mar-2018	225	32.84	18	87	13.375	83.45	10.625	1334.45	861,246.97	674,417.04	4,215.52	NNSS Survey 10/4/18
U-2ez SW20	20-Mar-2017	27-Mar-2017	27-Feb-2018	14-Mar-2018	225	65.68	18	85	13.375	81.40	10.625	1321.27	861,223.66	674,393.91	4,215.52	NNSS Survey 10/4/18
U-2ez SW40	23-Feb-2017	16-Mar-2017	19-Mar-2018	2-May-2018	225	131.14	18	86	13.375	83.80	10.625	1333.95	861,177.52	674,347.48	4,216.51	NNSS Survey 10/4/18
U-2ez SW80	12-Apr-2017	14-Apr-2017	10-Apr-2018	2-May-2018	225	262.43	18	85	13.375	83.68	10.625	1700.00	861,084.55	674,254.77	4,217.43	NNSS Survey 10/4/18

Note: Azimuth and distance from source hole refers to surface locations.

Elev = elevation
ft = feet
in. = inches
na = not applicable
NAD27 = North American Datum of 1927
NGVD29 = National Geodetic Vertical Datum of 1929
sft = U.S. survey feet
SPC = State Plane coordinate system (Nevada, Central, 2702)
TOC = top of casing

List of Attachments

1. Schalk, W., 2021. Written Communication prepared by the NNSS Weather Operations, Air Resources Laboratory/Special Operations and Research Division. *DAG Weather Data Collection*. Mercury, NV.
2. Vigil, J., 2021. *DAG Video Data Release*. Los Alamos National Laboratory Report LA-UR-21-24470. Los Alamos, NM.
3. Kelly, R., 2021. Written Communication prepared by Mission Support and Test Services, LLC. *High-Speed Video Camera and Handy-Cams*. Mercury, NV.

Attachment 1

Schalk, W., 2021. Written Communication prepared by the NNSS Weather Operations, Air Resources Laboratory/Special Operations and Research Division*. DAG Weather Data Collection*. Mercury, NV.

DAG Weather Data Collection

BACKGROUND

The surface weather data collected for the DAG experiments were from one temporary station and three stations in the SORD/NNSS Weather Mesonet. The Mesonet consists of 24 stations located all across the NNSS. The DAG data provided are from stations M09/A09AB, M49/A04AA, and M17/A01AB. These are 10-meter tall towers and are located approximately 2.5 km west-northwest, 6 km south-southeast, and 2.7 km southwest, respectively, from the DAG test bed. Wind observations and other weather observations, including temperature, humidity, atmospheric pressure, and solar radiation, were taken to provide 15-minute averaged data. The temporary station, M90, was a 2-meter tall station that recorded wind speed, wind direction, temperature, relative humidity, and atmospheric pressure every 2 seconds. This station was located approximately 2.5 km north-northwest of the DAG test bed. The SORD weather stations are sited, installed, operated, and maintained according to the ANSI/ANS-3.11 (2015) Voluntary Consensus Standard, "Determining Meteorological Information at Nuclear Facilities".

SURFACE DATA COLLECTION METHODOLOGY

The tables below summarize the collection methodology for the surface data collected. Table 1 defines how all of the observations from a standard NNSS Mesonet Weather tower are taken for the 15-minute averaged data on the 10-meter towers. Table 2 defines how the observations are taken for the 2-second data at a SORD/NNSS Micronet 2-meter portable tower.

Table 1: Weather Sensor Collection Methodology for Routine 15-minute Averaged Data, 10-meter tower

Parameter	Sensor	Location	Sample Rate	Data Processing	Units
15 minute Wind Speed	R.M. Young 3D 81000RE, Sonic Anemometer	10 meters, top of tower	4 times per second	Averaged over 15 minutes	Meters/ second
15 minute Wind Direction	R.M. Young 3D 81000RE, Sonic Anemometer	10 meters, top of tower	4 times per second	Averaged over 15 minutes	Compass Degrees
15 minute Wind Sigma Theta	R.M. Young 3D 81000RE, Sonic Anemometer	10 meters, top of tower	4 times per second	Averaged over 15 minutes	Compass Degrees
15 minute Wind Speed Maximum-Gust	R.M. Young 3D 81000RE, Sonic Anemometer	10 meters, top of tower	4 times per second	Maximum 3-second running average over the 15 minute period	Meters/ second
15 minute Wind Speed Minimum-Lull	R.M. Young 3D 81000RE, Sonic Anemometer	10 meters, top of tower	4 times per second	Minimum 3-second running average over the 15 minute period	Meters/ second

Table 1 continued: Weather Sensor Collection Methodology for Routine 15-minute Averaged Data, 10-meter tower

Parameter	Sensor	Location	Sample Rate	Data Processing	Units
15 minute Temperature-Upper	Vaisala HMP155A	8.5 meters, near top of tower	4 times per minute	Averaged over 15 minutes	Degrees Celsius
15 minute Relative Humidity-Upper	Vaisala HMP155A	8.5 meters, near top of tower	4 times per minute	Averaged over 15 minutes	% (percent)
15 minute Temperature-Lower	Vaisala HMP155A	2 meters, near bottom of tower	4 times per minute	Averaged over 15 minutes	Degrees Celsius
15 minute Relative Humidity-Lower	Vaisala HMP155A	2 meters, near bottom of tower	4 times per minute	Averaged over 15 minutes	% (percent)
15 minute Atmospheric Pressure	Vaisala Barometer PTB110-BCA	2 meters, near bottom of tower	4 times per minute	Averaged over 15 minutes	hecto-Pascals
15 minute Solar Radiation	Hukseflux Pyranometer LP02	2 meters, near bottom of tower	4 times per minute	Averaged over 15 minutes	W/m^2
15 minute Total Solar Radiation	Hukseflux Pyranometer LP02	2 meters, near bottom of tower	4 times per minute	Totaled over 15 minutes	kJ/m^2
15 minute Total Precipitation	Hydrological Services Tipping Bucket Rain Gauge TB3/P	Near Ground, opening about 1 meter AGL	Records “bucket” (0.01”) tips as occurs	Totaled over 15 minutes	inches
15 minute Battery Voltage	Campbell Scientific CR1000 Data Logger	In All-Weather Box at 1.5 meters	4 times per minute	Averaged over 15 minutes	Volts DC
15 minute Dew Point Temperature	N/A	2 meters, near bottom of tower	4 times per minute	Calculated from lower Temperature and Relative Humidity	Degrees Celsius
15 minute Delta Temperature with Height	N/A	Difference between 8.5m and 2m temperature	4 times per minute	Calculated from upper and lower Temperature	Degrees Celsius / meter
DataLogger	Campbell Scientific CR1000 Data Logger	In All-Weather Box at 1.5 meters	N/A	Collects and stores all data and transmits to Main PC	N/A

Table 2: Weather Sensor Collection Methodology for 2-second Data, 2-meter portable tower

Parameter	Sensor	Location	Sample Rate	Data Processing	Units
Battery Voltage	Campbell Scientific CR1000 Data Logger	In All-Weather Box at 1.5 meters	Once per second	Reported every 2 seconds	Volts DC
Minimum Battery Voltage	Campbell Scientific CR1000 Data Logger	In All-Weather Box at 1.5 meters	Once per second	Reported every 2 seconds	Volts DC
Wind Direction	Vaisala WXT520 Sonic Anemometer	At 2.0 meters, top of tripod	Once per second	Reported every 2 seconds	Meters / second
Wind Speed	Vaisala WXT520 Sonic Anemometer	At 2.0 meters, top of tripod	Once per second	Reported every 2 seconds	Meters / second
Temperature	Vaisala WXT520 Capacitive Ceramic THERMOCAP	At 2.0 meters, top of tripod	Once per second	Reported every 2 seconds	Degrees Celsius
Relative Humidity	Vaisala WXT520 Capacitive thin film polymer HUMICAP	At 2.0 meters, top of tripod	Once per second	Reported every 2 seconds	% (percent)
Pressure	Vaisala WXT520 Capacitive Silicone BAROCAP	At 2.0 meters, top of tripod	Once per second	Reported every 2 seconds	hectoPascals
Precipitation	Vaisala WXT520 Impact Sensitive piezo-electrical RAINCAP	At 2.0 meters, top of tripod	As occurs	Reported every 2 seconds	inches
DataLogger	Campbell Scientific CR1000 Data Logger	In All-Weather Box at 1.5 meters	N/A	Collects and stores all data and transmits to Main PC	N/A

RADIOSONDE (BALLOON) DATA COLLECTION METHODOLOGY

The table below summarizes the collection methodology for the upper air data (radiosonde/balloon) collected. Table 3 defines how the observations were taken. Measurements are taken by the radiosonde every 1 second and reported every 2 seconds.

Table 3: Radiosonde (Weather Balloon) Data Collection Methodology

Parameter	Sensor	Sample Rate	Data Processing	Units
Wind Speed	InterMet Radiosonde, iMet-1-ABx GPS	Once per second	Computed by the change in GPS position. Reported every 2 seconds	Meters/ second
Wind Direction	InterMet Radiosonde, iMet-1-ABx GPS	Once per second	Computed by the change in GPS position. Reported every 2 seconds	Compass Degrees
Temperature	InterMet Radiosonde, iMet-1-ABx Glass Bead	Once per second	Reported every 2 seconds	Degrees Celsius
Relative Humidity	InterMet Radiosonde, iMet-1-ABx Capacitive Polymer	Once per second	Reported every 2 seconds	% (percent)
Pressure	InterMet Radiosonde, iMet-1-ABx	Once per second	Reported every 2 seconds	hectoPascals
Location	InterMet Radiosonde, iMet-1-ABx GPS	Once per second	Reported every 2 seconds	Latitude (degrees)
Location	InterMet Radiosonde, iMet-1-ABx GPS	Once per second	Reported every 2 seconds	Longitude (degrees)
Location	InterMet Radiosonde, iMet-1-ABx GPS	Once per second	Reported every 2 seconds	Height (meters)

No challenges were encountered, data were collected as planned, and the results were as expected.

Please refer any questions and comments to Walt Schalk, Director, NOAA ARL/SORD at 702-295-1231, schalk@nv.doe.gov, walter.w.schalk@noaa.gov .

Attachment 2

Vigil, J., 2021. *DAG Video Data Release*. Los Alamos National Laboratory Report LA-UR-21-24470. Los Alamos, NM.

DAG Video Data Release

PI: Juan-Antonio Fidel Vigil, LANL J-NV

Video description:

Site camera footage was collected during each DAG experiment event to witness the event occurrence, and to record the degree to which the cables, from which each was suspended in the U2ez hole, were disrupted by the events.

Videos collected by LANL included:

1. DAG-1 shot, collected with LANL's U2ez site camera (60 fps);
2. DAG-1 cable cutters, collected with a GoPro camera directed down the hole from above (60 fps + audio);
3. DAG-2 shot, collected with 2 GoPro cameras directed down the hole from above (24 fps and 30 fps, both with audio);
4. DAG-2 cable cutters, collected with LANL's U2ez site camera (21 fps);
5. DAG-3 shot, collected with LANL's U2ez site camera (21 fps);
6. DAG-3 shot, collected with 2 GoPro cameras directed down the hole from above (120 fps + audio);
7. DAG-3 cable cutters, collected with LANL's U2ez site camera (30 fps);
8. DAG-3 cable cutters, collected with 2 GoPro cameras directed down the hole from above (120 fps, + audio);
9. DAG-4 shot, collected with LANL's U2ez site camera (24 fps);
10. DAG-4 shot, collected with a GoPro camera directed along the ground toward ground zero (60 fps + audio);

DAG Video Data Description:

Videos for DAG come in two varieties: shot videos and cable cutter videos. Shot videos were collected during the DAG experiments, which were nitromethane detonations at 1 ton, 50 tons, 1 ton, and 10 tons for DAG-1 through DAG-4 respectively. Each experiment was suspended from a pair of wire cables and installed in the U2ez hole at NNSS. The hole was stemmed with sand and grout above each experiment prior to detonation, so the cables show minimal motion due to the shot blasts. DAG-4 was installed very near the top of the U2ez hole, so the cables were not present above the hole once stemming material had cured. Cable cutter videos were collected during ancillary explosive operations that followed DAG-1, DAG-2, and DAG-3; each operation utilized small shaped charges with Comp C4 to cut the cables just above the stemming from each of the main tests. There was more motion of the cables during the cable cutter operations due to the release of tension that was applied during installation of the main DAG charges.

A total of 13 videos are ready for release as part of DAG project data reporting. Some were collected using LANL's U2ez site camera, and some with GoPro cameras. A sample frame from each video is given in the figures below, and the videos are available on request.

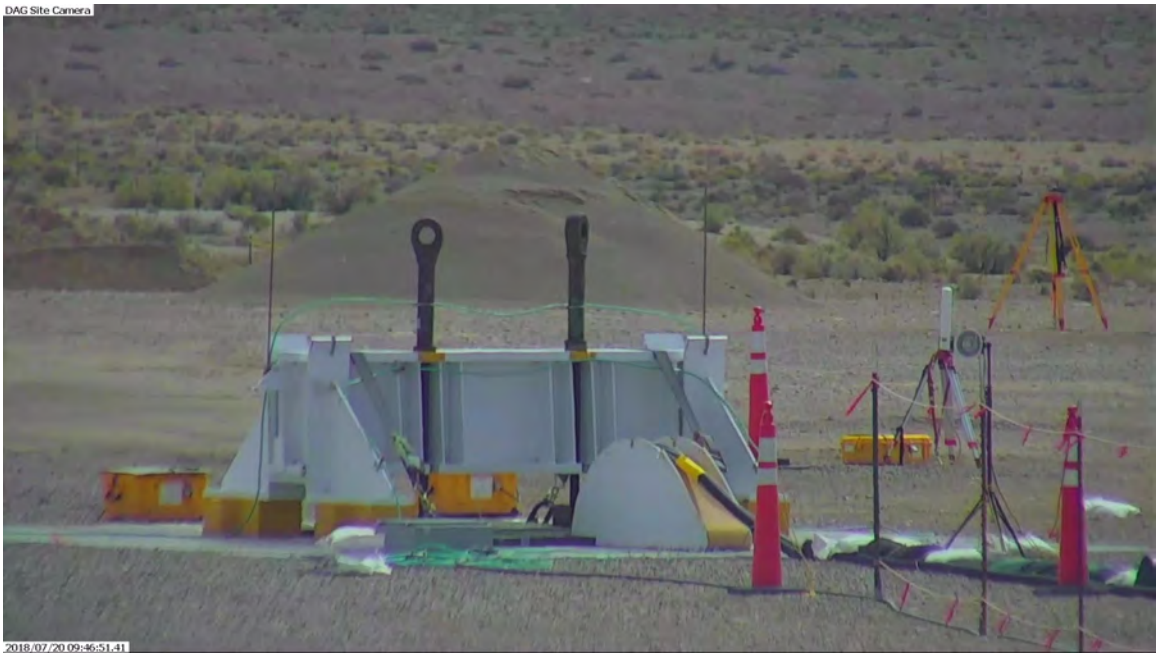

Figure 1. DAG-1 shot from the site camera; camera shake indicates the shot occurred.

Figure 2. DAG-1 cable cutters from a GoPro directed down the U2ez hole; dust is launched from the cables when tension is released.

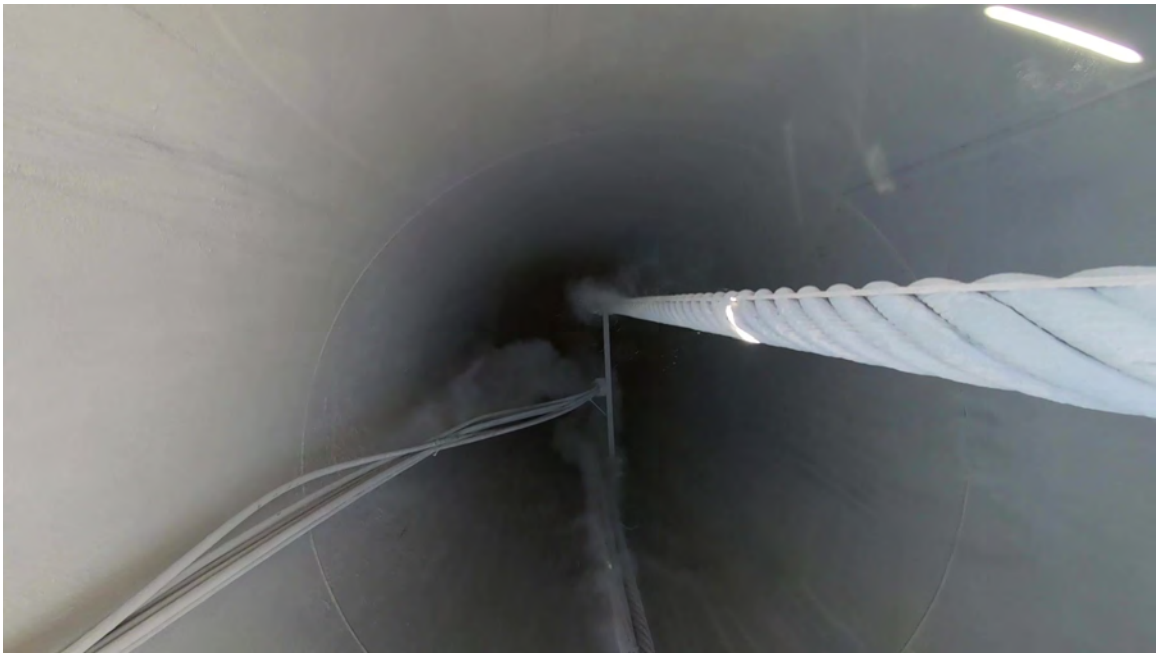

Figure 3. DAG-2 shot from GoPro 1, directed down the U2ez hole; dust is released from the cables due to the explosive blast.

Figure 4. DAG-2 shot from GoPro 2, directed down the U2ez hole; dust is released from the cables due to the explosive blast.

Figure 5. DAG-2 cable cutters from the site camera; cable "hop" can be seen as tension is released from the wires.

Figure 6. DAG-3 shot from the site camera; camera shake indicates the shot occurred.

Figure 7. DAG-3 shot from GoPro 1; debris is knocked from the cables by the explosive blast.

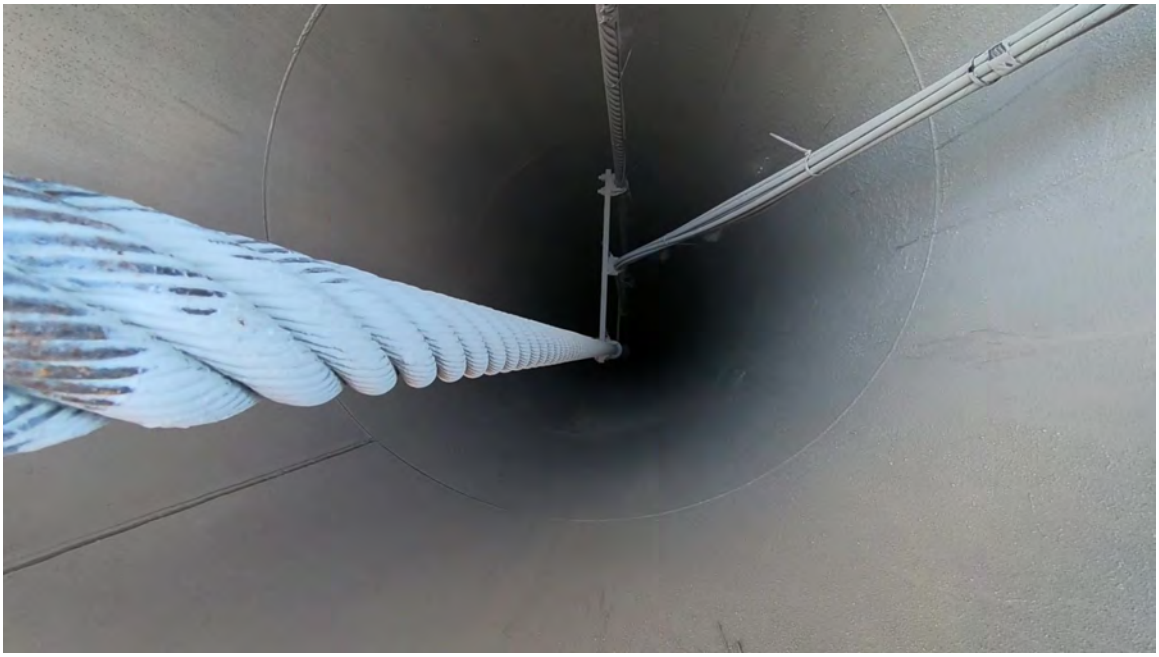

Figure 8. DAG-3 shot from GoPro 2; debris is knocked from the cables by the explosive blast.

Figure 9. DAG-3 cable cutters from the site camera; camera shake indicates shot occurred.

Figure 10. DAG-3 cable cutters from GoPro 1; debris is knocked from the cables when tension is released.

Figure 11. DAG-3 cable cutters from GoPro 2; debris is knocked from the cables when tension is released.

Figure 12. DAG-4 shot from the site camera; minor ground heave due to the blast launches dust from the ground.

Figure 13. DAG-4 shot from a GoPro; minor ground heave due to the blast launches dust from the ground.

Attachment 3

Kelly, R., 2021. Written Communication prepared by Mission Support and Test Services, LLC. *High-Speed Video Camera and Handy-Cams*. Mercury, NV.

"High-Speed Video Camera and Handy-Cams"

Provided By: Rand Kelly

Fielding Support: Michael Hanache, Kaleb Howard, James Wilson

MSTS fielded two (2) high-speed Phantom V711 cameras (S/N: 11894 and S/N: 13546) and four (4) handy-cams (HC-01, HC-02, HC-03, and HC-04) for each of the DAG experiments and also the cable cutter events. The goal of fielding both high-speed and low-speed video was to capture any ground motion, determine estimates of shock propagation, determine symmetry of shock propagation, and also record any late-time events that may have occurred at U-2ez and the surrounding area from different vantage points.

Both high-speed video cameras were located West of U-2ez in a large enclosure (we called the "Ice Box") that was temperature controlled and had a viewport on the side of it covered by plexiglass so no wind or debris would interrupt the view of the cameras. It also housed all of the equipment necessary to communicate with the systems remotely from the BEEF trailer park. In order to mitigate any sort of ground vibration coming from the equipment so it would not affect the seismic recording equipment around U-2ez, all of the equipment in the Ice Box trailer were running either off of a RUPS unit or dedicated battery supplies for the high-speed cameras. The handy-cams were positioned roughly North, East, West, and at U-2ez at varying distances depending upon the event itself.

Figure 1: Trailer (Ice Box) to house high-speed cameras and other equipment.

Figure 2: Close up view of both Phantom high-speed cameras on top of our optical bread board for stabilization. In-between is one of our handy-cams.

Figure 3: View from HC-01 East of U-2ez.

A total of 36 videos were collected from DAG I, DAG II, DAG II Cable Cutters, DAG III, DAG III Cable Cutters, and DAG IV. All videos are available upon request from Rand Kelly (kellyrp@nv.doe.gov).

PHANTOM HIGH-SPEED VIDEO CAMERAS						
SHOT	CAMERA (S/N)	LOCATION	LENS (mm)	FRAME RATE (fps)	RESOLUTION	EXPOURE TIME (µs)
DAG I	11894	ICE BOX WEST OF U-2EZ	100	8,300	1280 x 720	90
DAG I	13546	ICE BOX WEST OF U-2EZ	200	8,300	1280 x 720	90
DAG II	11894	ICE BOX WEST OF U-2EZ	100	8,300	1280 x 720	90
DAG II	13546	ICE BOX WEST OF U-2EZ	200	8,300	1280 x 720	90
DAG II Cable Cutter	11894	ICE BOX WEST OF U-2EZ	100	8,300	1280 x 720	90
DAG II Cable Cutter	13546	ICE BOX WEST OF U-2EZ	200	8,300	1280 x 720	90
DAG III	11894	ICE BOX WEST OF U-2EZ	105	8,300	1280 x 720	100
DAG III	13546	ICE BOX WEST OF U-2EZ	180	8,300	1280 x 720	100
DAG III Cable Cutter	11894	ICE BOX WEST OF U-2EZ	105	8,300	1280 x 720	110
DAG III Cable Cutter	13546	ICE BOX WEST OF U-2EZ	180	8,300	1280 x 720	100
DAG IV	11894	ICE BOX WEST OF U-2EZ	180	8,300	1280 x 720	100
DAG IV	13546	ICE BOX WEST OF U-2EZ	58	8,300	1280 x 720	100

Table 1: Phantom High-Speed Video Camera Locations and Settings

HANDY-CAM VIDEO CAMERAS			
SHOT	CAMERA (HC-XX)	LOCATION	FRAME RATE (fps)
DAG I	01	North East of U-2ez	24
DAG I	02	North West of U-2ez	24
DAG I	03	At U-2ez Looking Down Hole	24
DAG I	04	West of U-2ez in Ice Box	24
DAG II	01	North East of U-2ez	24
DAG II	02	North West of U-2ez on 2nd Stage	24
DAG II	03	At U-2ez Looking Down Hole	24
DAG II	04	North West of U-2ez	24
DAG II Cable Cutter	01	North East of U-2ez	24
DAG II Cable Cutter	02	North West of U-2ez on 2nd Stage	24
DAG II Cable Cutter	03	At U-2ez Looking Down Hole	24
DAG II Cable Cutter	04	North West of U-2ez	24
DAG III	01	East of U-2ez	24
DAG III	02	West of U-2ez Near Ice Box	24
DAG III	03	North of U-2ez	24
DAG III	04	At U-2ez Looking Down Hole	24
DAG III Cable Cutter	01	East of U-2ez	24
DAG III Cable Cutter	02	West of U-2ez Near Ice Box	24
DAG III Cable Cutter	03	North of U-2ez	24
DAG III Cable Cutter	04	At U-2ez Looking Down Hole	24
DAG IV	01	North West of U-2ez	24
DAG IV	02	North East of U-2ez	24
DAG IV	03	West of U-2ez in Ice Box	24
DAG IV	04	East of U-2ez (Balloon Hill)	24

Table 2: Handy-Cam Video Camera Locations and Settings

The analysis from the high-speed videos and the handy-cams indicate the following:

- DAG I
    - Surface shock propagation was calculated to be approximately 5.39 km/s.
    - Surface vertical displacement appears to be approximately 2.7 inches.
    - Geometry of surface shock appears to be radially symmetric from U-2ez.
- DAG II
    - Surface shock propagation was calculated to be approximately 6.70 km/s.
    - Surface vertical displacement appears to be approximately 4.6 inches.
    - Geometry of surface shock appears to be non-radially symmetric and displaced from U-2ez.
- DAG II Cable Cutters
    - No noticeable surface disturbance at U-2ez or extending from there.
    - Only noticeable movement were the large ring-hole bolts that appears to have vertically moved approximately 4.6 inches at U-2ez.
- DAG III
    - Surface shock propagation was calculated to be approximately 5.086 km/s.
    - Surface vertical displacement appears to be approximately 3.2 inches.
    - Geometry of surface shock appears to be radially symmetric and displaced from U-2ez.
- DAG III Cable Cutters
    - No noticeable surface disturbance at U-2ez or extending from there.
    - Only noticeable movement were a couple of cables at U-2ez.
- DAG IV
    - Surface shock propagation was calculated to be approximately 4.972 km/s.
    - Surface vertical displacement shows a large movement of approximately 8.0 inches.
    - Geometry of surface shock appears to be radially symmetric and centered at U-2ez.